Cyclic Universes & Direct Detection of Cosmic Expansion by Holonomy in the McVittie Spacetime

Mariam Campbell

A dissertation submitted in fulfillment

of the requirements for the degree of

Master of Science

at the

University of Cape Town

under the supervision of

Professor Peter K. S. Dunsby.

Department of Mathematics and Applied Mathematics

University of Cape Town

July 2, 2019

Plagiarism Declaration

I, Mariam Campbell, student number CMPMAR009, confirm that the work presented in this thesis is my own. Where information has been derived from other sources, I confirm that this has been referenced in the work.

Signature: Signed by candidate

Mariam Campbell

Date: _____

Abstract

This dissertation consists of two parts. They are separate ideas, but both fall into the context of General Relativity using dynamical systems. Part one is titled *Cyclic Universes*. It is shown that a Friedmann model with positive spatial sections and a decaying dark energy term admits cyclic solutions which is shown graphically by the use of phase planes. Coupling the modified Friedmann model to a scalar field model with cross-sectional terms in order to model the reheating phase in the early universe, it is found that there is a violation of the energy condition, i.e. $|w| > 1$, when the universe is in the contracting phase and re-collapses again. We suspect that the cause for this violation is due to the asymmetry of the solution of w together with the cross-sectional terms at the bounce preceding slow-roll inflation. Part two is titled *Thought Experiment to Directly Detect Cosmic Expansion by Holonomy*. Two thought experiments are proposed to directly measure the expansion of the universe by the parallel transfer of a vector around a closed loop in a curved space-time. Generally, expansion would cause a measurable deficit angle between the vector's initial and final positions. Using the McVittie spacetime (which describes a spherically symmetric object in an expanding universe) as a backdrop to perform these experiments it is shown that the expansion of the universe can be directly detected by measuring changes in the components of a gyroscopic spin axis. We find these changes to be small but large enough ($\Delta S \sim 10^{-7}$) to be measured if the McVittie spacetime were a representation of our universe.

Acknowledgements

I would like to express my appreciation to my supervisor, Peter Dunsby, for his guidance and support throughout my studies. The opportunities he has given me during my two years as a graduate student, attending graduate courses locally and internationally has given me a deepened insight about cosmology.

To my collaborators, George Ellis, Rituparno Goswami and Tony Rothman from whom I have learnt so much about approaching research problems, I thank you. Learning from you has been a great pleasure.

I would like to thank my officemates for their support and a special thanks to doctoral students Miguel Méndez Isla, Francisco (Pepe) Maldonado Torralba, and postdoctoral fellow Dr. Jack Morrice for their wisdoms, senior advice, and coffee trips. They made tough days so much easier and their support has been invaluable to me.

I also want to thank the *National Research Foundation* for their financial assistance to complete my studies.

Lastly, to my parents, your unwavering support with all my choices to pursue this and your belief in me to see it through, I am immensely grateful for.

Contents

List of Figures

List of Tables

Acronyms

LIGO	Laser Interferometer Gravitational-Wave Observatory
CMB	Cosmic Microwave Background
LSS	Large Scale Structure
SN1a	Supernova Type 1a
MCMC	Markov chain Monte Carlo

Part I

CYCLIC UNIVERSES

The material presented in this part is in preparation for publication.

1. Introduction

1.1 Review

Little is known about the physics and nature of space-time before the Planck era. Since the simplest classical inflationary model has been excluded by Planck 2015 data [2], this result has become more troublesome for inflationary models. It suggests a more complicated inflaton potential which mainly drives inflation, with more parameters requiring fine-tuning. There is also the initial conditions problem in this inflationary model, and one of the biggest cosmological problems - the initial singularity.

Even though single field inflationary models are favoured by experimental data, with the release of the final Planck data strongly supporting slow roll models with a concave potential [3], it does not mean that this is the only model used to describe the early universe. With astronomy and experimental physics embarking on new frontiers and making ground-breaking discoveries, standard models best describing our universe are still falling short. Therefore, alternative theories explaining or describing the origin and evolution of our universe are still important. Unless there is observational evidence which rules out a specific model or theory, we should still be taking alternative models and theories seriously.

The idea of a cyclic universe is an alternative theory which attempts to bypass the singularity problem, naturally cause rapid expansion in the early universe without the need to invoke inflation, and proceed to evolve in a series of contractions and expansions.

In 1934, Richard Tolman considered the effect of entropy increase on a periodic

sequence of closed Friedmann-Robertson-Walker universes [4]. He found that an increase in entropy leads to growing radiation pressure, and hence an increase in the volume of each cycle of expansion. This well-known result has been used to show that we cannot be living in a universe that has undergone an infinite number of past cycles because the present level of radiation entropy in the universe is far lower than what might be. Tolman's conclusions in his paper were formalized and confirmed by Zel'dovich and Novikov in 1983 [5], however, they argued that since there was a minimum possible entropy level, our universe could have undergone only a finite number of past oscillations.

Re-iterating, one of the main motivations for a cyclic model of the universe is to avoid the initial cosmological singularity. One of the earliest attempts to avoid the cosmological singularity was by Parker and Fulling in 1973 [6]. They considered a closed Robertson-Walker geometry and a classical gravitational field minimally coupled to a quantized neutral scalar field with mass. Their main goal was to study the impact of quantum theory on the classical singularity theorems. What they found was that the quantum effects in their model lead to the violation of the energy conditions which enter the singularity theorems. Their numerical solutions showed the Friedmann-like collapse halted and converted to a Friedmann-like expansion. The escape from a singularity in their model is a quantum coherence effect which depended on certain phase relationships in the specification of the quantum state. However, from their study, it appears that the solutions do eventually collapse after completing another cycle, and their model does not provide evidence that quantum effects will always avoid gravitational collapse.

Cyclic universes of the Tolman type were still favoured until the discovery of the accelerated expansion of the universe in 1998 [7], which introduced the concept of dark energy. Prior to this discovery, Barrow and Dabrowski authored a paper called *Oscillating Universes* in 1995 [8], where they investigated the properties of cyclic closed universes in the presence of different matter fields with a cosmological constant, but assuming the total entropy of the universe increases after each cycle. In the absence of a cosmological constant, they recovered

Tolman's solutions. When including a positive cosmological constant, it was found that no matter how small its value, oscillations would end, and the universe would enter a final state of deSitter expansion. However, if the cosmological constant derived from a slowly decaying vacuum energy which decays completely, for instance into radiation, then the de Sitter expansion would end and be replaced by renewed oscillations of growing amplitude.

After the discovery of accelerated expansion and the fact that the standard model of cosmology accounted for this so well by including the vacuum energy term Λ, the Tolman approach to cyclic universes was abandoned. In 2001, it was revived by Khoury, Ovrut and Steinhardt with the introduction of *The Ekpyrotic Universe* [9]. They introduce a scenario of brane collisions which addresses the cosmological problems which inflation eliminates without invoking inflation. The work is predominantly within the context of M-theory. Their model is built on the assumption that the universe begins in a non-singular, infinite, empty, quasi-static state of high symmetry. Here, inflation is not needed at all, and the brane collisions account for the matter-radiation energy and primordial density perturbations. However, in the paper by Linde, *Inflationary Cosmology after Planck 2013* [10], which discusses alternative models to inflation, a few shortcomings and inconsistencies with the original Ekpyrotic model are mentioned. The most significant problem highlighted is that instead of the big bang predicted in the Ekpyrotic scenario, there was a big crunch, as found in *Pyrotechnic universe* by Kallosh, Kofman and Linde [11], and *BPS branes in cosmology* by the same authors, including Tseytlin [12]. A more promising variant of the Ekpyrotic model, proposed by Anna Ijjas in 2016 in the paper *Cyclic Anamorphic Cosmology* [13], combines standard inflation with the features of the original Ekpyrotic model. Consequently, the model looks like standard inflation for cosmological fluctuations whereas matter feels an Ekpyrotic bounce.

In 2002, Steinhardt and Turok proposed *A Cyclic Model of the Universe* [14], where they claim to present new cosmology consisting of an endless sequence of cycles of expansion and contraction without invoking inflation, also explaining the

role of dark energy in the cyclic scenario. Their model is reminiscent of Tolman's, but they assume a universe that is infinite and flat, instead of finite and closed. However, to cause the reversal from expansion to contraction, a negative potential energy is introduced. Their explanation for dark energy in the cyclic model comes about when the scalar field ϕ comes to rest in the radiation-dominated phase and remains nearly fixed thereafter until dark energy begins to dominate, which is the result of the potential energy density acting with negative pressure that causes the accelerated expansion we see today. They hypothesized that if sustained for "hundreds of e-folds or more", the cosmic acceleration can flatten the universe and dilute entropy, blackholes, and other debris created over the preceding cycle. Ultimately, the scalar field begins to roll back toward $-\infty$, driving the potential back to zero. In this paper, it is not specified from when or where the universe emerges, and it is only stated the "there is no beginning and there is no end". However, explaining the stages of cycles in their model, the evolution starts at the radiation phase and evolves until dark energy dominates. The bounce condition of dark energy acting as a negative pressure is invoked, and as a result a new cycle starts. Yet, there are still unanswered questions this model poses: How does the universe emerge and how does it "bounce" through a space-time singularity at the end of each cycle?

A more recent construction by George Ellis et.al., *The Emergent Universe* [15-16], provides a scenario of a singularity-free inflationary universe. It is modeled by a single minimally-coupled scalar field with a physically based potential which dominates the early times. It is a simple, closed inflationary model in which the universe starts from an Einstein static state and enters an expanding phase that leads to inflation followed by reheating and then a standard hot big bang, with a radius larger than the Planck length so as to avoid the quantum gravity regime. Inspired by *The Emergent Universe* and motivated by the essential role it plays in the construction of non-singular emergent oscillatory models which are past eternal, a recent study was done on the stability of the Einstein static universe in the context of Ellis' paper, but under the Generalized Uncertainty Principle (GUP)

effects from quantum gravity [17]. The authors showed that their solution, in the presence of a perfect fluid, is cyclically stable around a center equilibrium point and found that, from determining the allowed interval for the effect equation of state parameter, it is stable in the presence of ordinary matter plus a spin fluid with a negative energy density and negative pressure.

An interesting paper in 2010, *Evidences for bouncing evolution before inflation in cosmological surveys* [18], considers a model which is a parametrization of the primordial spectrum featuring a jump in the amplitude of the power spectrum due to having a nonsingular bounce preceding inflation. A combination of the available CMB, LSS, SN1a data placed an upper limit on the bounce parameters of their model. The authors used the MCMC technique to do a global fitting to constrain the bounce parameters and compared it to the current data. Their analysis led to the conclusion that a nonsingular bounce preceding inflation would happen quickly at a very high energy scale. Although, as suggested by the authors, it could hardly be tested directly by experiments.

So far, only isotropic models were mentioned. This is not entirely the true description of our universe. With large-scale structures and matter that is gravitationally attractive, our universe is considerably anisotropic. So, there is a need to understand what happens to cyclic universes that allow anisotropic expansion. In the 2017 paper *Cyclic Mixmaster Universes* [19], Barrow and Ganguly considered the most general universe that allows anisotropic expansion whilst retaining spatial homogeneity, the Mixmaster universe of Bianchi type IX. The Bianchi type IX models have been well studied in connection with their dynamical behavior near a singularity, on time intervals that include the zero of time. If a bounce at finite expansion radius is considered at this time, then there is no need to worry about this chaotic behavior. For this bounce to come into effect in the Mixmaster universe, a ghost field is introduced. It produces smooth bounces at finite minima to eliminate the chaotic oscillations, but has no significant effect on the expansion maxima. Adding a cosmological constant to their model displays the expected long-term behavior in cyclic cosmologies. Adding a positive

cosmological constant, however small, terminates oscillations and the expansion tends to the isotropic de Sitter expansion. On the other hand, including a negative cosmological constant recovers the simple bouncing model that experiences a finite, non-singular minimum at the end of each cycle due to the presence of a ghost field. One surprising feature of this model is that, unlike in an isotropic universe, the sign of the 3-curvature also changes with time. It starts off negative and so no expansion maxima occur, but continues until it is isotropic enough for the 3-curvature to become positive. Only then does this type of closed universe re-collapse, although it would do so anisotropically.
In another paper by Solomons et.al. *Bounce behaviour in Kantowski-Sachs and Bianchi cosmologies* [20], it was shown that other Bianchi models, specifically LRS Bianchi type I, III, and Kantowski-Sachs models do not show bounce behaviour without violating the reality condition for the momentum density, $\dot{\phi} \geq 0$, with the exception of closed Friedmann and Bianchi type IX models, such as Barrow and Ganguly's Mixmaster universes.
To summarise, the important features of a cyclic or non-singular bounce scenario are:

1. Consider a closed geometry, i.e $k = +1$, since this describes a universe with spherical spatial sections where expansion is preceded by contraction or violates the energy condition.

2. Attempting to get rid of the initial singularity would still leave one with having to do fine-tuning of the initial conditions. The authors of *The Emergent Universe*, and the original Ekpyrotic model, and even the *Cyclic Mixmaster Universes*, faced the problem of fine-tuning initial conditions.

3. The most important feature: the cosmological constant. As there is still no explanation for dark energy, and the standard cosmological model currently best describes our universe, there is no ignoring the cosmological constant. The only way to have a successful cyclic scenario is to consider a decaying dark energy term.

1.2 Motivation

In this section we consider one of the simple models - a closed Friedmann cosmology with a decaying dark energy term. To date, the Friedmann model is still the best model at predicting the cosmological parameters as found in observational data. Also, recent Planck data [21], taking temperature-only (TT) lensing into account, gives the curvature parameter as

$$\Omega_k = -0.005^{+0.016}_{-0.017}.$$

This does not rule out the possibility of positive spatial curvature which is needed for a re-collapse. Until the observational data becomes more conclusive, we would still have to take models describing closed universes seriously. To describe the evolution of the entire universe this model is coupled with a chaotic scalar field. It will undergo four phases: a hot big bang, a radiation phase, matter domination, and then a dark energy phase. The phase space is explored with stability analysis. Extending recent work of Ellis et al. [22], we resolve some of the issues regarding their model:

1. Their decaying dark energy model violates the energy condition (the effective equation of state to become $w > 1$ before the turn-around time).

2. Their cut-and-paste approach for each cosmological epoch leads to discontinuities in the derivatives of the scale factor at the boundaries between each epoch.

The first problem is corrected by constructing an effective equation of state which produces the correct physics, then integrate the conservation of energy equation to find the density of dark energy. The model presented in this paper is continuous, using a dynamical systems approach.
The conditions for a bounce for Friedmann-Lemaître-Robertson-Walker (FLRW) models:

$$\dot{a}(t_b) = 0, \quad \ddot{a}(t_b) > 0,$$

where $a(t)$ is the scale factor or expansion factor, and t_b is the time at the bounce. Since the Hubble rate, $H(t)$, is negative during the contracting phase, it must increase during the expanding phase. To achieve this, the violation of the strong energy condition

$$\rho + 3p \geq 0,$$

where ρ is the *matter* density and p is the pressure, is necessary. Assuming the energy density in a FLRW space-time is a perfect fluid with an effective equation of state of the form $p = w\rho$, an additional constraint at the bounce is found:

$$\begin{aligned} &\rho + 3w\rho < 0 \\ &\Rightarrow \quad w < -\frac{1}{3}. \end{aligned}$$

This condition motivates our need for a decaying dark energy term in the late universe.

1.3 Friedmann dynamics

The famous Einstein field equation proposed in 1917, in its most general form,

$$G_{\mu\nu} + \Lambda g_{\mu\nu} = \kappa T_{\mu\nu}, \tag{1.1}$$

relates the distribution of matter to the geometrical structure of the universe. $G_{\mu\nu}$ is the Einstein tensor which describes a pseudo-Riemannian manifold, Λ is the cosmological constant, $g_{\mu\nu}$ is the metric tensor, $T_{\mu\nu}$ is the stress-energy tensor and $\kappa \equiv 8\pi G/c^2$ is Einstein's gravitational constant, where G is the gravitational constant.

To obtain the field equations, Λ is set to zero since one of the requirements is that

the gravitational equations reduce to the free-space field equations when the stress-energy tensor, $T_{\mu\nu}$, is zero.
This gives:

$$G^{\mu}{}_{\nu} = R^{\mu}{}_{\nu} - \frac{1}{2}\delta^{\mu}{}_{\nu}R \tag{1.2}$$

$$= \kappa T^{\mu}{}_{\nu}, \tag{1.3}$$

where $R^{\mu}{}_{\nu}$ is the Riemann tensor and $R = g^{\mu\nu}R_{\mu\nu}$ is the Ricci scalar.
In order to study the overall universe, the matter distribution is treated as being completely homogeneous. The inhomogeneities observed are then treated as deviations from this smooth universe. If we assume a homogeneous and isotropic universe then by Einstein's equations it implies that the matter distribution should be homogeneous and isotropic as well. Observationally this is not true, the universe is fairly inhomogeneous, consisting of galaxies, clusters, etc. However, we ignore the inhomogeneities and assume that the matter distribution is described by a smoothed-out average density in studying the large-scale dynamics of the universe. This is supported by observing the cosmic microwave background which proves the high level of isotropy of the observable universe. The FLRW metric is an exact solution of Einstein's field equations describing a homogeneous, isotropic, expanding or contracting universe - a solution which has the best description of the universe we observe today. The FLRW metric which satisfies Eq. (1.2) is given by

$$ds^2 = -c^2dt^2 + a^2(t)\left(\frac{dr^2}{1-kr^2} + r^2d\Omega^2\right), \tag{1.4}$$

where c is the speed of light, $d\Omega^2 = d\theta^2 + \sin^2\theta d\phi^2$, and the spatial curvature k which takes on the values $k = -1, 0, 1$, an open, flat, or closed universe respectively.
Einstein's tensor, $G^{\mu}{}_{\nu}$, can be computed from this metric for a specified stress-energy tensor.

The assumption of homogeneity and isotropy gives $T^{\mu}{}_{\nu}$ as

$$T^{\mu}{}_{\nu} = \text{dia}[\rho(t), -p(t), -p(t), -p(t)].$$

This gives the temporal and spatial components of Einstein's tensor as:

$$G^{0}{}_{0} = \frac{3}{a^2(t)}[\dot{a}(t)^2 + k], \qquad G^{i}{}_{j} = \frac{1}{a(t)^2}[2a(t)\ddot{a}(t) + \dot{a}(t)^2 + k]\delta^{i}{}_{j}.$$

Thus equation (1.2) gives two independent equations,

$$H(t)^2 \equiv \left(\frac{\dot{a}(t)}{a(t)}\right)^2 = \frac{\kappa\rho(t)}{3} - \frac{k}{a^2(t)}, \qquad \textit{Friedmann equation} \tag{1.5}$$

$$\frac{\ddot{a}(t)}{a(t)} = -\frac{\kappa}{6}(\rho(t) + 3p(t)). \qquad \textit{Raychaudhuri equation} \tag{1.6}$$

Additionally, the continuity equation is derived by taking the gradient of the stress-energy tensor, $\nabla_{\mu} T^{\mu\nu} = 0$:

$$\dot{\rho}(t) + 3H(t)[\rho(t) + p(t)] = 0, \qquad \textit{continuity equation} \tag{1.7}$$

where $H(t) \equiv \dot{a}(t)/a(t)$ is defined as the Hubble parameter.
Together with the equation of state for a perfect fluid,

$$p(t) = w\rho(t), \tag{1.8}$$

the unknowns $a(t)$, $\rho(t)$, and $p(t)$ can be determined. The universe consists of several fluids, and if the energy exchange between them is negligible, all the fluids satisfy the continuity equation separately. Therefore, an equation of state for each fluid, $p_i = w_i\rho_i$, with $i = \{\text{radiation, matter, } \Lambda \text{ - vacuum}\}$ can be defined. The effective equation of state, w, is a constant and takes on the values $w = -1, 0, 1/3$, to obtain solutions to a Λ, matter, radiation dominated universe respectively.

It is useful to rewrite the Friedmann equation in dimensionless form, where the energy density parameters are introduced:

$$\Omega_X = \frac{\kappa\rho_X(t)}{3H(t)^2}, \quad \Omega_\Lambda = \frac{\Lambda}{3H(t)^2}, \quad \Omega_k = \frac{k}{H(t)^2 a(t)^2}, \tag{1.9}$$

where the subscript X represents the *matter* fluids, ie. radiation, baryons and cold-dark matter. This reduces the Friedmann equation to:

$$\sum_X \Omega_X + \Omega_\Lambda - \Omega_k = 1, \tag{1.10}$$

which will be referred to as the Friedmann constraint throughout this dissertation. In Chapter 2, we will dive into the dynamics of the Friedmann model and possible solutions describing different universes, and also explore how the dynamics changes when a decaying dark energy term is used which shows possible cyclic behaviour.

1.4 Scalar field dynamics

The fact that the Friedmann-Lemaître space-time provides a good description of the later periods of the universe in no way implies that it describes the primordial period of the universe.

In traditional primordial cosmology, our universe starts with a big bang and carries on in eternal expansion, although at a slower rate since after inflation gravitational effects of matter slows down the universe's expansion. The Big Bang model is a good standard model, however it is incomplete. Conclusions from the model are that the universe was dominated by radiation in the past, succeeded by a matter dominated era, the model depends on its matter content and the universe has a thermal history where it emerged from a state with high temperatures. However, the model does become less reliable entering this regime at about energies close to the Planck scale at 10^{19}GeV, where we would have to start considering quantum gravity effects.

To resolve the issues of homogeneity with the Big Bang model and the flatness problem, the concept of inflation was introduced - a period of rapid expansion

before the radiation era of the standard Big Bang model. The flatness problem concerns the unusual small value of the curvature term k/a^2 at the beginning of the universe predicted by the Big Bang model. With inflation, the curvature term decreases so much whereby its dynamical effect can be ignored and we effectively obtain $k = 0$. The horizon problem concerns the inability to explain the homogeneity of causally disconnected regions in the universe. Inflation resolves this by placing two regions in causal contact at the start of inflation and due to the rapid expansion, the comoving Hubble radius $(aH)^{-1}$ decreases with time resulting in these regions being separated by a distance larger than the Hubble radius. In 1981, Alan Guth [23] was the first to use inflation to solve cosmological problems. The following year, Linde made a new proposal of inflation and Guth's model has since been dubbed as *old inflation*. In Linde's model, inflation can start from a Planckian density even if the universe is not in a thermal equilibrium. The homogeneity and isotropy of our universe would then only be local properties while the universe is inhomogeneous on very large scales. This is a result of the slow-roll phase, an essential feature of Linde's model, where it is during this period that density fluctuations are generated which leads to the large-scale structures observed today.

Inflation is a phase during which the scale factor of the universe is accelerating, $\ddot{a}(t) > 0$. Immediately following from the Raychaudhuri equation, there is the condition $\rho(t) + 3p(t) < 0$. Since the energy density is always assumed to be positive, the pressure has to be negative to satisfy this condition. As such, scalar field dynamics is the key to understanding the inflationary epoch since it has the feature of a potential energy that may red-shift slowly as the universe expands which corresponds to an effective equation of state with a negative pressure. During inflation, fields are present as opposed to particles and the properties of any system is specified by its action. In the context of general relativity the action will be of the form:

$$S = \int d^4x\sqrt{-g}\mathscr{L}, \tag{1.11}$$

where $d^4x\sqrt{-g}$ is the volume element in generic coordinates and $\mathscr{L}$ is the Lagrangian density. For a scalar field, $\phi \equiv \phi(t)$, the Lagrangian density is:

$$\mathscr{L} = -\frac{1}{2}g^{\mu\nu}\partial_\mu\phi\partial_\nu\phi - V(\phi),$$

where $V(\phi)$ is the scalar potential of the field.

Varying $g_{\mu\nu}$ in the action gives the Einstein field equations with a stress-energy tensor:

$$T_{\mu\nu} = -2\frac{\partial\mathscr{L}}{\partial g^{\mu\nu}} + g_{\mu\nu}\mathscr{L}. \tag{1.12}$$

The pressure and energy density are then expressed in terms of the scalar field and scalar potential:

$$\rho_\phi = T_{00} = \frac{1}{2}\dot{\phi}^2 + V(\phi), \tag{1.13}$$

$$p_\phi = T_{ii} = \frac{1}{2}\dot{\phi}^2 - V(\phi). \tag{1.14}$$

Substituting Eq. (1.13) and Eq. (1.14) into the continuity equation (1.7) yields the scalar wave equation $(H = H(t))$:

$$\ddot{\phi} + 3H\dot{\phi} + \frac{\partial V}{\partial\phi} = 0. \tag{1.15}$$

This equation is the same as the classical equation of motion for a ball rolling down a hill with friction which is provided by the expansion of the universe. To include reheating of the universe another term has to be added, which does not follow from the Lagrangian, and provides damping of the oscillations:

$$\ddot{\phi} + 3H\dot{\phi} + \frac{\partial V}{\partial\phi} = -\Gamma_\phi\dot{\phi}, \tag{1.16}$$

where Γ_ϕ is the decay width of the ϕ particle. The radiation phase and pressure-less matter phase are included as separate fluids which are coupled to the inflationary model. The complete model then looks like:

$$\ddot{\phi} + 3H\dot{\phi} + \frac{\partial V}{\partial \phi} = -\Gamma_r \dot{\phi} - \Gamma_m \dot{\phi}, \tag{1.17}$$

$$\dot{\rho}_r + 4H\rho_r = \Gamma_r \dot{\phi}^2, \tag{1.18}$$

$$\dot{\rho}_m + 3H\rho_m = \Gamma_m \dot{\phi}^2, \tag{1.19}$$

$$\dot{H} = -H^2 + \frac{V(\phi)}{3} - \frac{\dot{\phi}^2}{3} - \frac{\rho_r}{3} - \frac{\rho_m}{6} + \frac{\rho_\Lambda}{3}, \tag{1.20}$$

$$\dot{K} = -2HK, \tag{1.21}$$

$$\dot{a} = aH, \tag{1.22}$$

where $K = k/a^2$ and the simplest quadratic potential, [†]$V(\phi) = 1/2m_\phi^2\phi^2$, is used as a toy model to simulate inflation. We decompose the reheating constant, Γ_ϕ, into $\Gamma_\phi = \Gamma_r + \Gamma_m$ so that the evolution of the radiation and matter density are coupled to the scalar field and in Chapter 3 we determine the value of these constants from cosmological data found today.

In the section which deals with an inflationary induced bounce by Ellis et al. [22], our model extends the authors' by including the evolution of radiation and matter. Since it is safe to assume that the radiation and matter densities are zero during the inflationary phase due to it being red-shifted away, it does not necessarily mean that their evolution equations can be ignored. Also, during this phase, the Λ density is taken to be a constant. It does not have a significant effect on the dynamics of the early universe, but it is included in the model for completeness as is the dynamical curvature term as well.

[†]Recent Planck data [2] disfavour this quadratic chaotic inflation model, and natural inflation at about 95% CL having strengthened the upper limits on the scalar-to-tensor ratio.

1.5 Outline

The outline of the proceeding sections is as follows:

In Chapter 2, the dynamical framework for the Friedmann model is introduced, following the conventions in [1]. An extension of this model is investigated where a dynamical dark energy term is considered, and an analysis of the phase-space is done. The same methodology is followed for the early universe, coupling the Friedmann model to a scalar field, where possible bounce behavior is shown in the phase space solution.

In Chapter 3, the scalar field dynamics including the reheating process in the early universe is addressed. We find that there is a violation of the energy condition, $w > 1$, during the contracting phase of an inflationary bounce. The reason for this violation is due to the asymmetry of the solution of w together with the cross-sectional terms which model the reheating phase. The initial conditions of the inflationary model are determined numerically using the values of the cosmological parameters as measured today, and the value of the reheating coefficients Γ_r and Γ_m. The bounce condition replaces the initial singularity and provides the initial conditions for the inflationary model which is compared to the conditions found from today's cosmological values.

It will be concluded with a discussion of results and future work this study could lead to in Chapter 4.

Lastly, the conventions used in this part, $c = \kappa = 1$ will be assumed.

2. Cyclic Universes: A Phase Plane Analysis

In this chapter we reformulate the Friedmann equations in the form of a dynamical system adapted to study cyclic scenarios and investigate its properties. In order to notice this, it is useful to rewrite the Friedmann and Raychaudhuri equations in terms of the dimensionless density parameters as defined by Eq. (1.9).

We follow the work of Goliath and Ellis [1] focusing on the Friedmann-Lemaître model in the $k = 1$ case. Their novel approach to studying this model is rich in information and shows the versatility of using a dynamical systems approach. They focused on understanding the dynamical evolution of the model only when $\Lambda > 0$ by constructing its state space. This model can easily be adapted by replacing the pure cosmological constant with a decaying term, which would result in a bounce during the late-time universe and showing cycles in the solution state space. This is done in Section 2.2, and a solution for a pure cosmological constant is recovered, as found in [1]. We also find the conditions which would result in a bounce in the early universe and the solution state space is a closed cycle.

The only notation different to the Goliath and Ellis paper is that we will use the effective equation of state, w, whereas they use the constant γ with its relation to the effective equation of state as $w = \gamma - 1$. By this relation, causality requires the interval of w to be $-1 \leq w \leq 1$.

2.1 Bounce conditions

Friedmann cosmologies for a closed spatial geometry ($k = 1$ case) allows for the Hubble parameter to vanish, i.e. $H = 0$. This allows the universe to re-collapse as H transitions from positive to negative values. Further, one can provide conditions at the bounce as a direct result from the Raychaudhuri equation:

$$\dot{H} > 0,$$
$$w_b < -\frac{1}{3}.$$

These conditions would describe a bounce from a collapsing to an expanding universe. However, during inflation w varies due to the oscillatory behaviour of the scalar field, and this could allow a solution to experience a bounce and a re-collapse. During inflation, it is safe to assume that the radiation and matter densities are zero since they are red-shifted away, so we can construct the effective equation of state at the bounce as:

$$w = \frac{\frac{1}{2}\dot{\phi}^2 - V(\phi)}{\frac{1}{2}\dot{\phi}^2 + V(\phi)}.$$

Imposing the global bounce condition, $w < -1/3$, gives an additional condition before the onset of slow-roll inflation, $\dot{\phi}^2 < V(\phi)$.
Before addressing the cyclic model with inflation, let us consider a model with pressure-less matter and a decaying dark energy.

2.2 A cyclic universe with pressure-less matter and a decaying dark energy

We will only be focusing on the case when $k = 1$ of the Goliath and Ellis model. The three-curvature is defined as ${}^3R = 6k/a^2$, and with $\kappa = 1$, the Friedmann equations become

$$H^2 = \frac{\rho_m}{3} - \frac{^3R}{6} + \frac{\rho_\Lambda}{3}, \tag{2.1}$$

$$\frac{\ddot{a}}{a} = -\frac{3w_m + 1}{6}\rho_m + \frac{\rho_\Lambda}{3}, \tag{2.2}$$

and the matter energy conservation equation:

$$\dot{\rho}_m = -3(w_m + 1)H\rho_m. \tag{2.3}$$

In our model, we will be replacing the constant Λ term with a decaying dark energy term where its effective equation of state is of the form

$$w_\Lambda = -1 + \frac{bx}{1+bx}, \tag{2.4}$$

$x \equiv a/a_0$, and b is a scaling constant so that the dark energy epoch occurs at the correct value of the scale-factor. In the domain $\{x : 0, \infty\}$, the range of the effective equation of state is $\{w_\Lambda : -1, 0\}$. Our decaying dark energy phenomenological model does not violate the energy conditions and addresses the problem with the Ellis et al. [22] phenomenological model.
Two additional evolution equations are obtained:

$$\dot{\rho}_\Lambda = -3\,(w_\Lambda + 1)\,H\rho_\Lambda, \tag{2.5}$$

$$\dot{w}_\Lambda = -w_\Lambda\,(w_\Lambda + 1)\,H. \tag{2.6}$$

Assuming $H \neq 0$, the dimensionless variables are defined as Eq. (1.9) and the Friedmann constraint is Eq. (1.10), where the subscript X will denote pressure-less matter in our case.
With $\rho_\Lambda \geq 0$ and the weak energy condition, which is

$$\rho \geq 0 \quad \text{and} \quad \rho + p \geq 0,$$

the following constraints are given

$$\Omega_\Lambda \geq 0, \quad \Omega_m \geq 0, \quad \Omega_k \geq -1.$$

Now for models with non-positive spatial curvature ${}^3R$, the range of these dimensionless quantities are in a compact interval:

$$0 \leq \Omega_\Lambda \leq 1, \quad 0 \leq \Omega_m \leq 1, \quad -1 \leq \Omega_k \leq 0.$$

However, we are interested in the case when $\Omega_k > 0$, which is not compact. In order to compactify this region, we note that Eq. (2.1) can be re-expressed as $\rho_m = 3H^2 + {}^3R/2 - \rho_\Lambda$. For models with ${}^3R > 0$, one can see that the dominant quantity is $D^2 = H^2 + {}^3R/6$. So D is used instead of H, to obtain compact variables for the $k = 1$ case. Additional dimensionless variables are defined:

$$Q = \frac{H}{D}, \quad \tilde{\Omega}_\Lambda = \frac{\Lambda}{3D^2}, \tag{2.7}$$

where the sign of Q indicates if a model is in an expanding or contracting phase. Redefining the time variable as $' = D^{-1}d/dt$, the evolution equations become

$$D' = -\frac{3}{2}\left(1 + w + (w_\Lambda - w)\,\tilde{\Omega}_\Lambda\right) QD, \tag{2.8}$$

$$Q' = \frac{3}{2}(Q^2 - 1)\left(w + \frac{1}{3} + (w_\Lambda - w)\tilde{\Omega}_\Lambda\right), \tag{2.9}$$

$$\tilde{\Omega}'_\Lambda = 3(w - w_\Lambda)Q(1 - \tilde{\Omega}_\Lambda)\tilde{\Omega}_\Lambda, \tag{2.10}$$

$$w'_\Lambda = -w_\Lambda(w_\Lambda + 1)Q. \tag{2.11}$$

The evolution equation for D is decoupled, i.e. there is no dependence on the variable D in Eqs. (2.9-2.11), so this reduces the system in terms of Q, $\tilde{\Omega}_\Lambda$ and w_Λ. The equilibrium points are $(Q, \tilde{\Omega}_\Lambda, w_\Lambda) = (\pm 1, 0, -1)$ and $(Q, \tilde{\Omega}_\Lambda, w_\Lambda) = (\pm 1, 1, -1)$, when $w_m = 0$. They correspond to the flat Friedmann and de Sitter solutions respectively. Each model has an expanding and contracting

solution. For $-1 < w_\Lambda < 0$, there is an additional equilibrium point, given by

$$Q = 0, \quad \tilde{\Omega}_\Lambda = -\frac{1}{3w_\Lambda}, \tag{2.12}$$

which has a saddle stability for values $-1 \leq w_\Lambda < -0.4$ and a center otherwise, as tabulated in Table (2.1). The equilibrium point representative of the Einstein static solution implies that $\dot{a} = 0$, $\ddot{a} = 0$. This satisfies the bounce condition that $w_\Lambda < -1/3$ and $H = 0$ which means $\Omega_m \to \infty$.

When $w_\Lambda = -1$, for a constant dark energy term, the Einstein static point in the Goliath and Ellis paper is recovered, see Fig. (2.2). With a decaying dark energy term an additional equilibrium point is obtained which represents a center in the phase space, creating the possibility for cyclic universes. Fig. (2.2) shows that if our universe were situated in the Goliath and Ellis submanifold (a universe with a constant cosmological constant), one would stay in this subspace as $w_\Lambda = -1$ is also a fixed point. So in order to enter a cyclic universe one needs a decaying dark energy. However, it is interesting in this regard that a decaying dark energy term shows this behavior in the phase-space, as in the Goliath and Ellis model when they consider $-1 < w < -1/3$ for their matter-energy content, there is no longer an equilibrium point corresponding to the Einstein static universe, see Fig. (2.1b).

Solution	Fixed points $(Q, \tilde{\Omega}_\Lambda, w_\Lambda)$	Stability
Friedmann (F)	$(-1,0,-1)$	sink
	$(1,0,-1)$	source
deSitter (dS)	$(-1,1,-1)$	saddle
	$(1,1,-1)$	saddle
Einstein static (E)	$(0,1/3,-1)$	saddle
	$(0,-1/3w_\Lambda, w_\Lambda)$	$-1 \leq w_\Lambda < -0.4$, saddle
Cyclic solution (C)	$(0,1,-1/3)$	center
	$(0,-1/3w_\Lambda, w_\Lambda)$	$w_\Lambda = -0.4$, center

Table 2.1: Stability analysis of the modified system, (2.9)-(2.11).

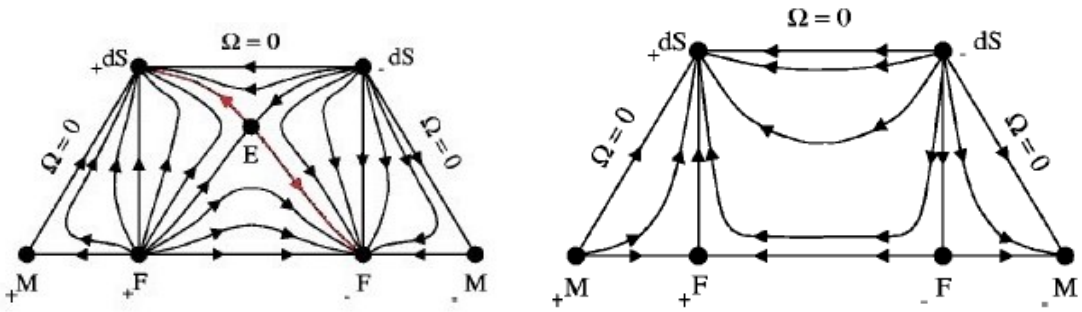

Figure 2.1: The state space taken from Goliath and Ellis [1]. The rectangular regions in the phase space correspond to models with $k > 0$ and the triangular regions correspond to $k < 0$ models. Fig. (a) shows the phase space for $-1/3 < w < 1$ and the $k > 0$ region is recovered in Fig. (2.2) for a constant cosmological constant. Fig. (b) shows the phase space for $-1 < w < -1/3$ where there is no longer an Einstein static equilibrium point.

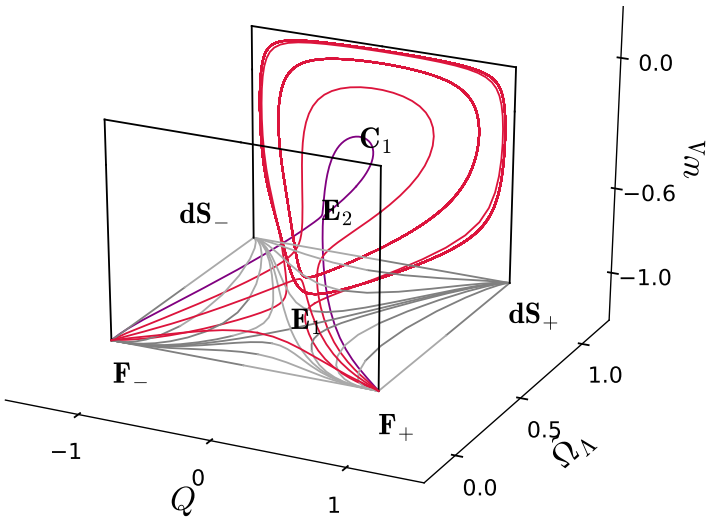

Figure 2.2: State space for FL models with a decaying dark energy term and EoS for matter set to $w = 0$. There is an additional equilibrium point corresponding to the Einstein static universe E_2, when w_Λ obeys the bounce condition which is, in this case, $w_\Lambda < -1/3$. The solution found in [1] is recovered for a constant cosmological *constant* in the $w_\Lambda = -1$ plane, as expected.

Next, we have a look at a possible cyclic scenario using cosmological data.

2.2.1 A possible cyclic scenario including the radiation phase with today's density content

In this section, the evolution equations in the previous Section 2.2 are updated to include the radiation phase. A phase space is constructed using the cosmological parameter values found in the 2015 Planck Data [21] as initial values:

$$\Omega_{r,0} = 9.281 \times 10^{-5}, \qquad \Omega_{m,0} = 0.315, \qquad \Omega_{\Lambda,0} = 0.685,$$
$$\Omega_{k,0} = 0.005, \qquad w_{\Lambda,0} = -0.92.$$

The following subscripts denote the energy densities $\{r, m, \Lambda\}$=$\{$radiation, matter, dark energy$\}$ and the subscript k is the curvature of our universe, as measured today, indicated by the subscript 0. The initial value for Q after a little algebraic manipulation from its definition Eq. (2.7) and the definition for D, is
$Q_0 = 1/\sqrt{1+\Omega_{k,0}} = 0.9975$.
The system of equations including radiation are:

$$Q' = \left(Q^2 - 1\right)\left[\Omega_r + \frac{1}{2}\Omega_m + \frac{1}{2}\left(1 + 3w_\Lambda\right)\Omega_\Lambda\right], \tag{2.13}$$

$$\Omega_r' = -2Q\Omega_r\left[1 - \Omega_r - \frac{1}{2}\Omega_m - \frac{1}{2}\left(1 + 3w_\Lambda\right)\Omega_\Lambda\right], \tag{2.14}$$

$$\Omega_m' = -Q\Omega_m\left[1 + 2\left(-\Omega_r - \frac{1}{2}\Omega_m - \frac{1}{2}\left(1 + 3w_\Lambda\right)\Omega_\Lambda\right)\right], \tag{2.15}$$

$$\Omega_\Lambda' = -3\left(1 + w_\Lambda\right)Q\Omega_\Lambda - 2Q\Omega_\Lambda\left[-1 - \Omega_r - \frac{1}{2}\Omega_m - \frac{1}{2}\left(1 + 3w_\Lambda\right)\Omega_\Lambda\right], \tag{2.16}$$

$$w_\Lambda' = -w_\Lambda\left(1 + w_\Lambda\right)Q. \tag{2.17}$$

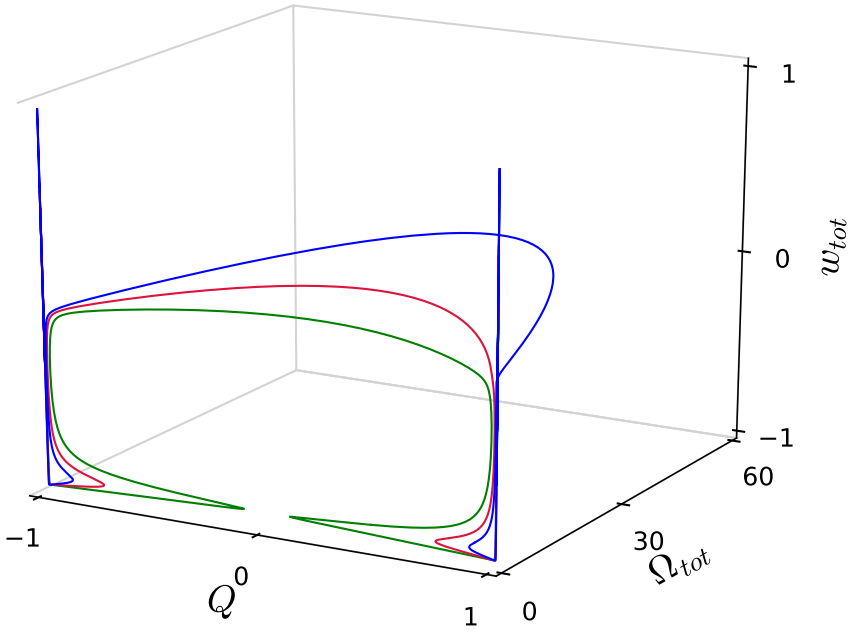

Figure 2.3: State space solutions for different values of Q_0 with the *matter* content fixed to the values found today. The blue curve corresponds to the solution with the value of Q_0 today.

As can be seen from the phase plot Fig. (2.3), all curves pass through the point which defines our universe today, so they are also possible cyclic scenarios. The values for the total energy density, Ω_{tot}, are greater than 1 since we are considering a phase space with spherical spatial sections, i.e. $k = +1$. For a flat universe ($k = 0$), the total energy density would equal 1.

Let us now turn our attention to models which include an inflationary epoch.

2.3 Building a complete cyclic model which includes inflation

To achieve a cyclic universe, a scalar field is coupled to the Friedmann model with a decaying dark energy term. The scalar field would describe the inflationary epoch. Rewriting the Friedmann equation in the form $\dot{a}^2 + U_{eff} = -k$, Fig. (2.4) gives an illustration as to how to achieve a cyclic universe by means of the effective potential, $U_{eff} = -a^2(\rho + \rho_{de})$.

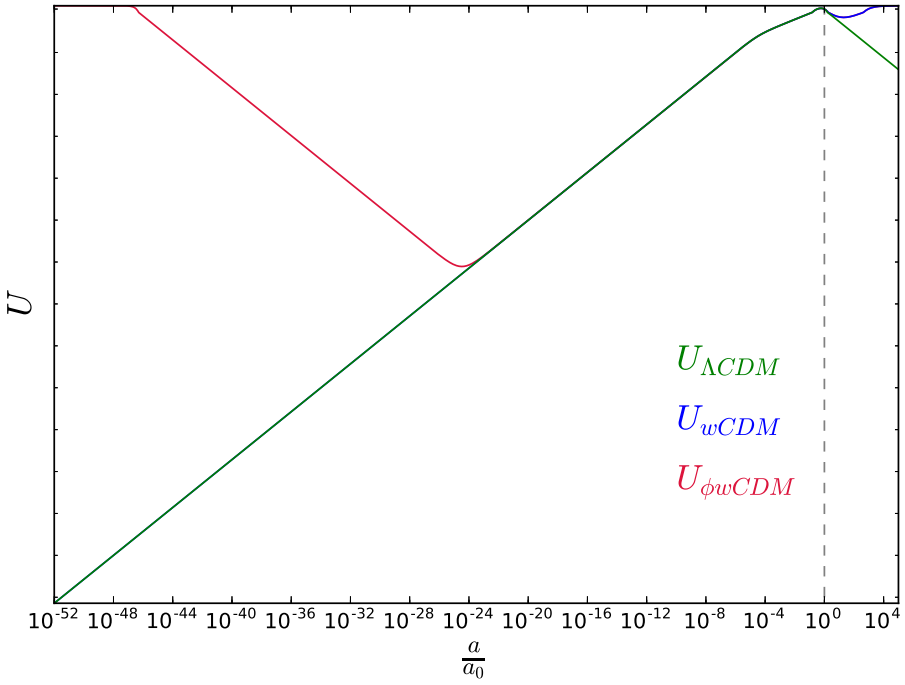

Figure 2.4: How a cyclic universe can be achieved by replacing Λ with a decaying dark energy term, U_{wCDM}, and then completing the cycle by coupling the Friedmann model to a single scalar field ϕ, $U_{\phi wCDM}$.

The density ρ_{de} is the dark energy density found from our decaying dark energy phenomenological model Eq. (2.4). The epochs, inflation, radiation and matter are modeled into the ρ term by introducing the following effective equation of state:

$$w = -1 + \frac{4\left(\frac{x}{c}\right)}{1+3\left(\frac{x}{c}\right)} - \frac{\left(\frac{x}{d}\right)}{1+3\left(\frac{x}{d}\right)}, \tag{2.18}$$

where $x = a/a_0$ and, c and d are scaling constants so that each cosmological epoch begins at the correct value of the scale-factor. We construct a phase portrait of $\dot{a} = \pm\sqrt{x^2(\rho + \rho_{de}) - 1}$, for different values of the scale-factor a, see Fig. (2.5).

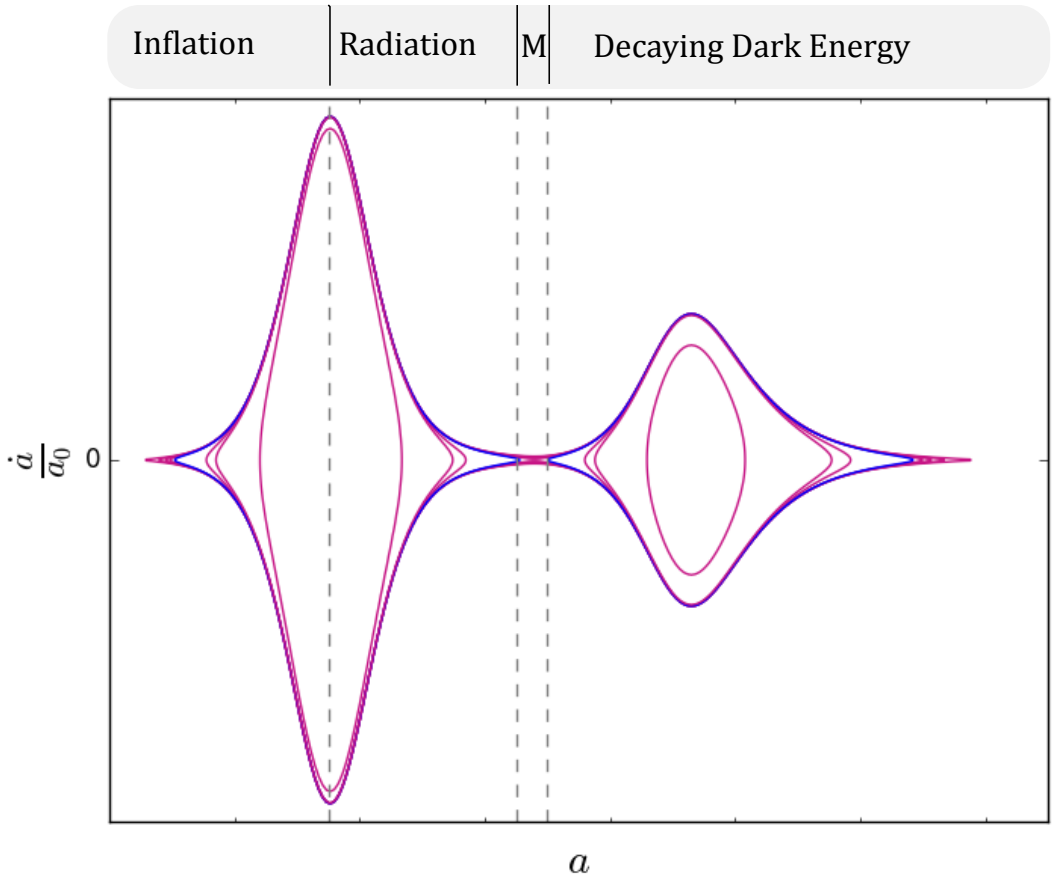

Figure 2.5: Constructing the effective potential with the following epochs in a cyclic scenario: inflation, radiation, pressure-less matter (labeled M) and decaying dark energy. This plot is produced for different values of the scale-factor a with the density values fixed to the ones found today. The blue curve is when $a = 1$ – today. This figure is not to scale since a transformation function had to be applied to $\dot{a}$ to compress the solution curves in order to see the entire evolution in a single figure.

This graphical representation of a cyclic universe fits in with what is found in Ellis et al. [22]. However, our construction is continuous and avoids the problem of discontinuities in the derivatives of the scale-factor, as in [22].

Let us now consider a model with actual inflationary physics, where we will model the inflationary phase using scalar field dynamics.

2.4 A cyclic model in the early universe with a scalar field and radiation

In this case, we model a self-gravitating scalar field and radiation density, excluding the cross-sectional terms ($\Gamma_i\dot{\phi}^2$) which model the reheating phase for now. To compactify the phase space, the following dynamical variables are introduced:

$$\tilde{\Omega}_\phi = \frac{\rho_\phi}{3D^2}, \qquad\qquad \tilde{\Omega}_r = \frac{\rho_r}{3D^2}.$$

The Raychaudhuri equation in this case is expressed as

$$\dot{H} + H^2 = -\frac{\rho_\phi}{6}\left(1+3w_\phi\right) - \frac{\rho_r}{6}\left(1+3w_r\right). \tag{2.19}$$

The following dynamical system is then derived, where the dimensionless derivative is defined as $' = D^{-1}d/dt$.

$$D' = -\frac{Q}{2}D\left[\tilde{\Omega}_\phi\left(1+3w_\phi\right) + \tilde{\Omega}_r\left(1+3w_r\right) + 2\right], \tag{2.20}$$

$$Q' = \frac{1}{2}\left(Q^2-1\right)\left[\tilde{\Omega}_\phi\left(1+3w_\phi\right) + \tilde{\Omega}_r\left(1+3w_r\right)\right], \tag{2.21}$$

$$\tilde{\Omega}_\phi' = Q\tilde{\Omega}_\phi\left[\tilde{\Omega}_\phi\left(1+3w_\phi\right) + \tilde{\Omega}_r\left(1+3w_r\right) - 9w_\phi - 1\right], \tag{2.22}$$

$$\tilde{\Omega}_r' = Q\tilde{\Omega}_r\left[\tilde{\Omega}_\phi\left(1+3w_\phi\right) + \tilde{\Omega}_r\left(1+3w_r\right) - 2\right], \tag{2.23}$$

where $w_r = 1/3$ and the effective equation of state for the scalar field is $w_\phi = p_\phi/\rho_\phi$, with the scalar field density and pressure defined by Eq. (1.13) and Eq. (1.14) respectively. The potential $V(\phi) = 1/2m_\phi^2\phi^2$ is used as a toy model. Since there is now a dependence on ϕ and $\dot{\phi}$, two additional equations are required to complete the dynamical system:

$$\dot{\phi} = X(t), \tag{2.24}$$

$$\dot{X} = -3QDX - m_\phi^2\phi. \tag{2.25}$$

From the bounce conditions in Section (2.1), we can determine the initial condition for $\dot{\phi}$. By constructing the effective equation of state at the bounce and imposing the bounce conditions, we find

$$\dot{\phi}^2 = \frac{\phi^2(w_b+1) - 2\rho_r(1/3 - w_b) + 2\rho_\Lambda(w_b+1) + 2w_b\rho_m}{1-w_b}. \tag{2.26}$$

Choosing $w_b = -0.6$, which satisfies the bounce condition $w_b < -1/3$, and $Q_i = 0$ ($H = 0$) at the bounce results in the following phase space solution:

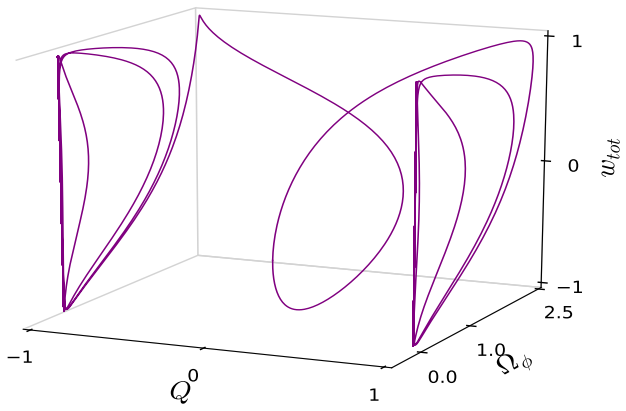

Figure 2.6: State space solution for a self-gravitating scalar field and radiation density. The initial values are such that the scalar field is dominant in the evolution, $\tilde{\Omega}_\phi = 0.7$ and $\tilde{\Omega}_r = 0.3$. Here we can see that the universe would undergo a single bounce at $Q = 0$.

Our solution shows that with a dominant scalar field in the early universe, the bounce is asymmetrical. The same conclusion is reached in Chapter 3 without the phase plane analysis. This differs from the solution in [22] where the authors find a symmetrical bounce. This is discussed further in the following chapter.

3. A Bounce in the Early Universe

In this chapter, the conditions at the start of the reheating phase is found using the values of the cosmological parameters as measured today. We find the solution to an inflationary bounce, with and without reheating, and compare it to the conditions found at the reheating phase with today's cosmological data.

We would like to find the bounce conditions before inflation that would give us the cosmological parameters of today as found in the 2015 Planck data [21]. The first step is to find the conditions at the beginning of the radiation phase. The Klein-Gordon equation Eq. (1.17) which is used to model the inflationary epoch is ignored and the Γ's in the subsequent expressions Eq. (1.18) and Eq. (1.19) are inactive, i.e. set to zero.

The system excluding the inflationary model is integrated backwards to the point where the radiation phase began. The second step is to include the inflationary model. During the inflationary epoch there are two phases: the *slow-roll* regime proceeded by the *coherent oscillations* regime, as in Kolb and Turner [24]. In the slow-roll regime, $\ddot{\phi}$ is negligible and the $\Gamma_\phi \dot{\phi}$ particle creation term is inactive. The coherent oscillations regime is when significant particle production takes place. This is only possible when the scalar field undergoes rapid oscillations about its global minimum, resulting in the kinetic term $\dot{\phi}^2$ to oscillate sinusoidally, and can be replaced by its average over an oscillation cycle. The coherent oscillations regime is described by the evolution Eqs. (3.7)–(3.12), and its dimensionless form Eqs. (3.13)–(3.18). During this epoch there are tighter constraints on our model so we assume that the initial values of the matter and radiation densities are zero since it would be red-shifted away. This system is integrated forward, to match the

conditions found at the start of the radiation phase. Lastly, the conditions for a bounce before the onset of the slow-roll regime are tied into the conditions found at the point when particle production takes place during inflation.

3.1 Conditions at the beginning of the radiation phase

In *The Early Universe* by Kolb and Turner [24], the end of inflation occurred at $T \sim 10^{27}K$. This gives us an approximate value of the scale-factor at the end of inflation which is $a_{end} \simeq T_0/T = 2.71 \times 10^{-27}$, where $T_0 = 2.71K$ is the temperature measured today.

Using the conditions of today as initial conditions, and no decaying dark energy term, the system of equations are integrated backwards to find the conditions at the beginning of the radiation phase. For stability of the numerical code, the system of equations are re-written in dimensionless form:

$$\Omega_r' = -4\Omega_r - 2\Omega_r[-1 - \Omega_r - \frac{1}{2}\Omega_m + \Omega_\Lambda], \tag{3.1}$$

$$\Omega_m' = -3\Omega_m - 2\Omega_m[-1 - \Omega_r - \frac{1}{2}\Omega_m + \Omega_\Lambda], \tag{3.2}$$

$$\Omega_k' = -2\Omega_k - 2\Omega_k[-1 - \Omega_r - \frac{1}{2}\Omega_m + \Omega_\Lambda], \tag{3.3}$$

$$a' = a, \tag{3.4}$$

$$H' = H[-1 - \Omega_r - \frac{1}{2}\Omega_m + \Omega_\Lambda], \tag{3.5}$$

where $\Omega_\Lambda = 1 - \Omega_r - \Omega_m + \Omega_k$, as from the Friedmann constraint, and the dimensionless time derivative is redefined as $' \equiv H^{-1}d/dt$. This dimensionless time derivative is reintroduced to stabilize the numerical integration. The initial conditions for this system are:

$$\Omega_{r0} = 9.281 \times 10^{-5}, \qquad \Omega_{m0} = 0.315 \pm 0.013, \qquad \Omega_{k0} = 0.005^{+0.016}_{-0.017},$$
$$a_0 = 1, \qquad H_0 = 67.31 \pm 0.96.$$

The conditions at the end of inflation can also be determined analytically by the following expressions for the densities and the dimensionless Hubble parameter:

$$h^2 = \left(\frac{H}{H_0}\right)^2 = \Omega_{r0}\left(\frac{a}{a_0}\right)^{-4} + \Omega_{m0}\left(\frac{a}{a_0}\right)^{-3} + \Omega_{\Lambda 0} - \Omega_{k0}\left(\frac{a}{a_0}\right)^{-2},$$

$$\frac{\Omega_r}{\Omega_{r0}} = \left(\frac{a}{a_0}\right)^{-4}\left(\frac{H_0}{H}\right)^2, \qquad \frac{\Omega_m}{\Omega_{m0}} = \left(\frac{a}{a_0}\right)^{-3}\left(\frac{H_0}{H}\right)^2,$$
$$\frac{\Omega_k}{\Omega_{k0}} = \left(\frac{a}{a_0}\right)^{-2}\left(\frac{H_0}{H}\right)^2, \qquad \frac{\Omega_\Lambda}{\Omega_{\Lambda 0}} = \left(\frac{H_0}{H}\right)^2.$$

The numerical and analytical results are tabulated in Table 3.1.

Parameter	Numerical Result	Analytical Result
a	2.715×10^{-27}	2.71×10^{-27}
Ω_r	1	1
Ω_m	9.215×10^{-24}	9.485×10^{-24}
Ω_k	3.971×10^{-52}	4.05006×10^{-52}
h	1.307×10^{51}	1.292×10^{51}

Table 3.1: Values of the cosmological parameters at the end of inflation when performing the numerical backward integration, and comparing these results to the analytical expression for the ΛCDM cosmology.

3.2 Coherent oscillations regime

During inflation, the evolution is purely driven by the scalar field, ϕ. So Ω_r and Ω_m are set to zero as an initial condition, and other forms of energy densities like dark energy are ignored. This is a reasonable approximation since these densities rapidly red shift away during the inflationary phase. The density ρ_ϕ can be approximated to $\rho_\phi \simeq \langle \dot{\phi}^2 \rangle$ during the coherent oscillations regime. For a simple harmonic oscillator $\langle V \rangle = \langle \dot{\phi}^2/2 \rangle = \rho_\phi/2$, we find that $\langle p_\phi \rangle = \langle \dot{\phi}^2/2 - V(\phi) \rangle$ vanishes and the coherent oscillations behave like non-relativistic matter. It is useful to multiply Eq. (1.16) by $\dot{\phi}$ and rewrite it as

$$\dot{\rho_\phi} + 3H\dot{\phi}^2 = -\Gamma_\phi \dot{\phi}^2.$$

Replacing $\dot{\phi}^2$ by its average over an oscillation gives

$$\dot{\rho_\phi} + 3H\dot{\phi}^2 = -\Gamma_\phi \rho_\phi. \tag{3.6}$$

The evolution equations are expressed as

$$\dot{\rho_\phi} + 3H\rho_\phi = -\Gamma_r \rho_\phi - \Gamma_m \rho_\phi, \tag{3.7}$$

$$\dot{\rho_r} + 4H\rho_r = \Gamma_r \rho_\phi, \tag{3.8}$$

$$\dot{\rho_m} + 3H\rho_m = \Gamma_m \rho_\phi, \tag{3.9}$$

$$\dot{K} = -2HK, \tag{3.10}$$

$$\dot{H} = -H^2 - \frac{\rho_\phi}{6} - \frac{\rho_r}{3} - \frac{\rho_m}{6}, \tag{3.11}$$

$$\dot{a} = aH. \tag{3.12}$$

For the numerical integration, they are re-expressed in dimensionless form, where $\Omega_\phi \equiv \rho_\phi / 3H^2$:

$$\Omega'_\phi = -4\Omega_\phi - 2\Omega_\phi[-1 - \frac{1}{2}\Omega_\phi - \Omega_r - \frac{1}{2}\Omega_m] - \frac{\Gamma_r}{H}\Omega_\phi - \frac{\Gamma_m}{H}\Omega_\phi, \tag{3.13}$$

$$\Omega'_r = -4\Omega_r - 2\Omega_r[-1 - \frac{1}{2}\Omega_\phi - \Omega_r - \frac{1}{2}\Omega_m] + \frac{\Gamma_r}{H}\Omega_\phi, \tag{3.14}$$

$$\Omega'_m = -3\Omega_m - 2\Omega_m[-1 - \frac{1}{2}\Omega_\phi - \Omega_r - \frac{1}{2}\Omega_m] + \frac{\Gamma_m}{H}\Omega_\phi, \tag{3.15}$$

$$\Omega'_k = -2\Omega_k - 2\Omega_k[-1 - \frac{1}{2}\Omega_\phi - \Omega_r - \frac{1}{2}\Omega_m], \tag{3.16}$$

$$a' = a, \tag{3.17}$$

$$H' = H[-1 - \frac{1}{2}\Omega_\phi - \Omega_r - \frac{1}{2}\Omega_m]. \tag{3.18}$$

Evolving this set of equations, 60 e-folds is used in order to achieve successful inflation. From the number of e-foldings, the scale-factor at which inflation begins, $a_i = e^{-60} a_{end}$, is also determined. As before, $a_{end} \simeq 2.71 \times 10^{-27}$. The initial conditions to solve the system Eqs. (3.13)–(3.18) are fine-tuned to obtain the cosmological parameter values at the start of the radiation phase which should correspond to the cosmological parameter values as found in the previous Table 3.1. The results are tabulated in Table 3.2, with the decay constants set to $\Gamma_r = 1.75 \times 10^{54}$, and $\Gamma_m = 3.94 \times 10^{30}$.

Parameter	Initial condition	Result at the end of inflation	Comparison to Table 3.1
a	2.373×10^{-53}	2.707×10^{-27}	2.71×10^{-27}
Ω_ϕ	1	0.000126	0
Ω_r	0	0.9999286	1
Ω_m	0	9.486×10^{-24}	9.485×10^{-24}
Ω_k	8.488×10^{-79}	4.0804×10^{-52}	4.08006×10^{-52}
h	3.231×10^{90}	1.2918×10^{51}	1.29176×10^{51}

Table 3.2: At the onset of inflation, these are the initial conditions required to match the values found at the end of inflation, transitioning into the radiation-dominated epoch.

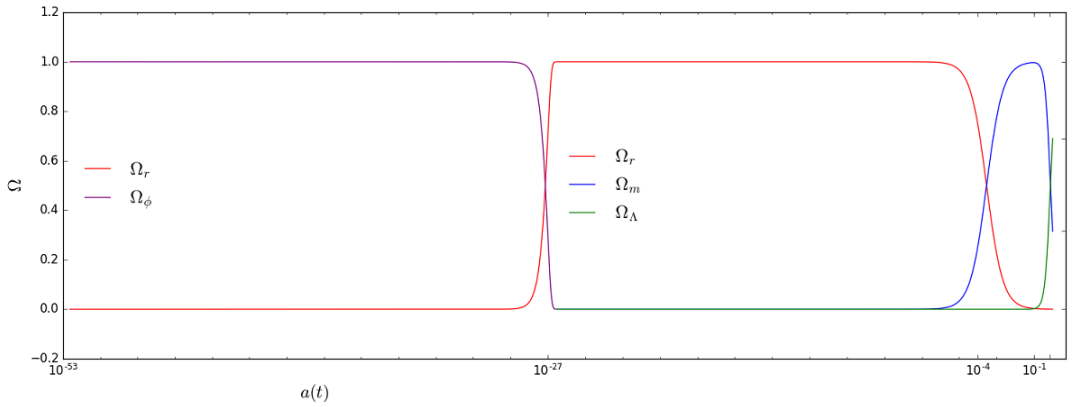

Figure 3.1: This is a plot of the dimensionless densities when the ΛCDM model is coupled to a scalar field including the process of reheating. The Ω_ϕ density (purple curve) is when the inflaton is oscillating about its potential minimum after the slow-roll phase. During $a(t) \sim 10^{-53} - 10^{-27}$, the scalar field is dominant and the density ρ_ϕ behaves as pressureless matter. At around 10^{-27}, the radiation density becomes dominant, so Γ_r and Γ_m are zero, and the densities evolve according to the ΛCDM model. The red curve represents the radiation density, Ω_r, the blue curve represents pressure-less matter Ω_m, and the green curve represents dark energy Ω_Λ.

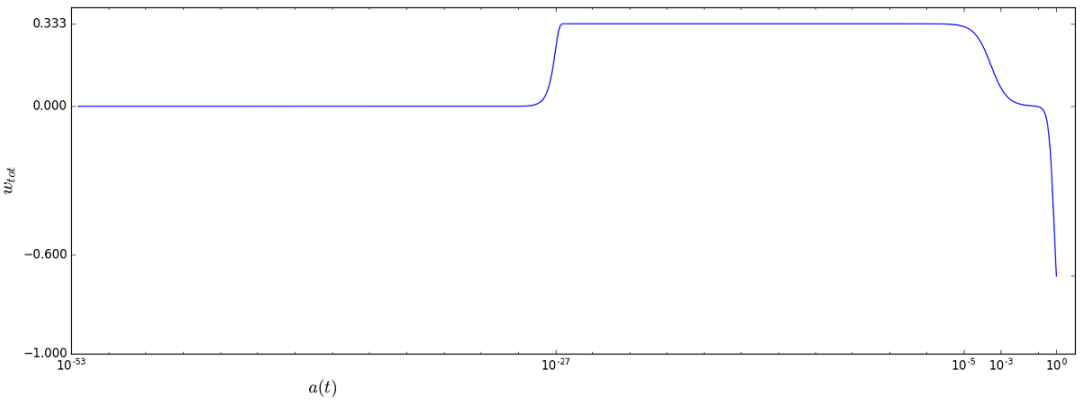

Figure 3.2: This figure shows the total effective equation of state. Here, one can see that while the inflaton is oscillating about its potential minimum, the scalar density acts as pressure-less matter.

We now turn our attention to slow-roll inflation preceded by a bounce, with and without a reheating phase, and see if the solutions tie in with the conditions found in this section.

3.3 Slow-roll inflation preceded by a bounce

Numerically solving the system of equations (1.17)–(1.22), without the reheating phase, i.e. $\Gamma_r = \Gamma_m = 0$, the initial conditions are placed at the bounce. It is then evolved away from the bounce point for an expanding solution. Due to the temporal symmetry of the equations, evolving back would result in the same profile but it would then describe a collapsing solution, as illustrated in [22]. We find that the early universe would undergo a bounce and quickly enter a phase of slow-roll inflation. However, unlike the result found in [22], the bounce is not symmetric since our total effective equation of state includes the radiation and matter densities, as shown in Fig. (3.3).

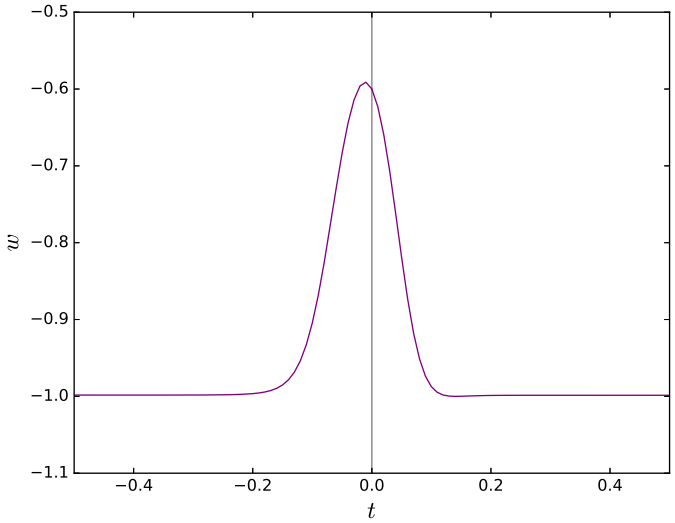

Figure 3.3: The total effective equation of state for an inflationary induced bounce.

The initial conditions needed to produce this bounce only depend on the bounce requirement that $H = 0$, $w < -1/3$, and the initial value of the potential, which can be determined by the number of e-foldings necessary to achieve enough inflation. These conditions are all in agreement with current data. The inflationary singularity theorems, proposed by Guth [23], exclude the case of positive spatial curvature – a universe that is allowed to contract and the possibility that $H_i = 0$. Since our model considers these cases, the inflationary singularity theorems need not apply.

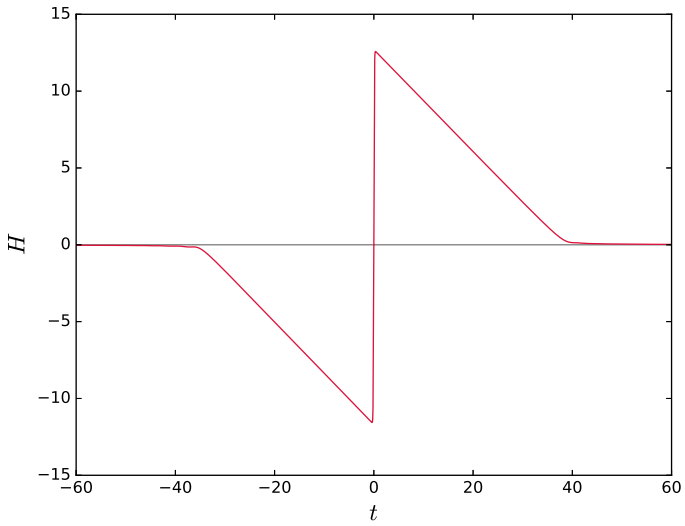

Figure 3.4: The solution to the Hubble parameter at the bounce shows that it would experience a symmetrical bounce.

3.4 Including reheating to an inflationary induced bounce

We proceed to include the process of reheating to our inflationary model, i.e. Γ_r and Γ_m are nonzero. The initial conditions are once again placed at the bounce and then evolved away. During the slow-roll regime, the term $\Gamma_\phi \dot{\phi}$ is inactive and is switched on at a later time. This is done numerically by multiplying the reheating terms $\Gamma_r \dot{\phi}$ and $\Gamma_m \dot{\phi}$ by a rectangular pulse function which has the conditions:
If the integration time t is in the interval $-50 < t < 50$ (this interval need not be that long since after the bounce the universe quickly enters the slow-roll phase, as seen in the previous section) then the rectangular pulse function equals zero. Outside this integration interval, the rectangular pulse function equals 1, that is when the reheating phase takes effect.
Since the evolution from the bounce to the start of the radiation phase is over a short period of the scale-factor, the solution is in terms of the numerical integration time. For illustration purposes, the values of Γ_r and Γ_m were set to smaller values, see Fig. (3.5). However, this shows that for any nonzero value of Γ_i there would be a violation of the energy condition.

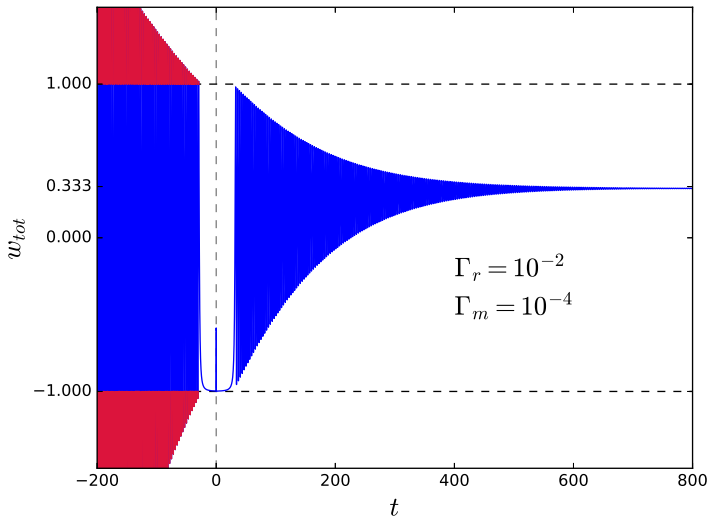

Figure 3.5: The total effective equation of state for an inflationary induced bounce with reheating. The solution is oscillatory but cannot be seen since it is oscillating rapidly over the integration interval. The left-hand side of the solution, describing a contracting universe, shows the violation of the energy condition, $|w_{tot}| > 1$.

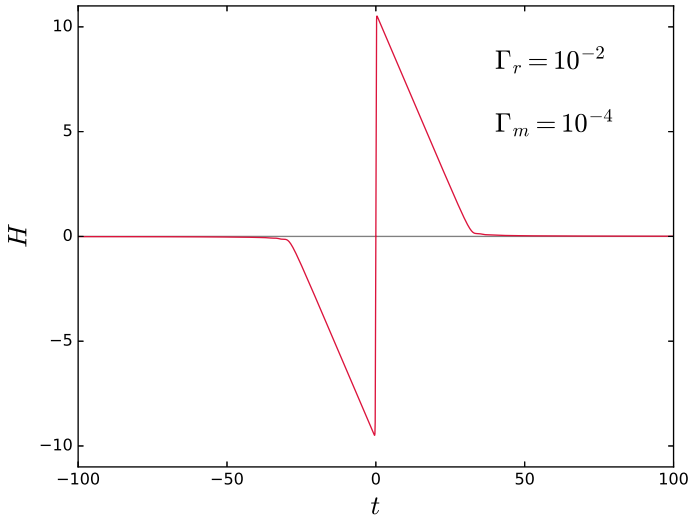

Figure 3.6: The Hubble parameter including reheating. The effects of reheating are close to negligible in the solution to the Hubble parameter as it resembles closely to the solution found without the effect of reheating, see Fig. (3.4).

In summary, this section is an extended and complete analysis of an inflationary induced bounce by [22]. Including the process of reheating, which connects inflation to the standard model, we found that there is a violation of the energy

condition, $|w| > 1$. This could be a result of the asymmetry of the bounce together with the reheating terms.

4. Discussion

After a bounce, the universe's density goes through the reversal description of its matter state during expansion. What this would mean is interesting in the context of physics. The bounce would be followed by a phase of anti-pressureless matter, anti-radiation, cooling instead of reheating and anti-inflation, back to a bounce.

Including the process of reheating to our model produced interesting results. When the universe undergoes contraction, there is a violation of the energy condition. This could be due to the asymmetry of the bounce together with the terms modeling reheating. There is no physical explanation for this, the model may not be adequate and other models of the reheating process need to be explored. Admittedly, the process of reheating in the early universe is not that well understood and this would be interesting to explore further.

Other extensions of this model is to include a bulk viscosity term such that the late-time evolution would dampen and settle on an Einstein static solution. In the phase space solution this would correspond to seeing a spiral instead of cycles in the late-time universe. This would be future work, and it would also be interesting to do an extension of this model in the framework of modified gravity.

Part II

THOUGHT EXPERIMENT TO DIRECTLY DETECT COSMIC EXPANSION BY HOLONOMY IN THE MCVITTIE SPACETIME

This part contains material from Ref. [25] which I co-authored on: Tony Rothman, Mariam Campbell, Rituparno Goswami, George F.R. Ellis, *Direct Detection of Universal Expansion by Holonomy in the McVittie Spacetime* (Aug 2018, revised version Jan 2019). Published as a Regular Article in *Physical Review D*.

5. Introduction

Investigations into how the large-scale behaviour of the universe affects local physics have been ongoing for just over seven decades. This kind of inquiry was inspired by Einstein since he tried to incorporate Mach's principle into general relativity. He then followed in this line of work with Strauss [26], where they modeled a Schwarzschild domain in an expanding universe in order to understand how expansion would affect the local physics.

More recent papers following this theme include Bochicchio and Faraoni [27], where they examine how a FLRW universe affects the behaviour of a Lemaître-Tolman-Bondi system; Faraoni and Jacques [28], where they examine whether various systems embedded in a FLRW universe plays a role in the expansion; Cooperstock, Faraoni and Vollick [29], where they inquire as to how the universal expansion of an FLRW universe affects the equations of motion in a local inertial frame.

McVittie was one of the earliest people to undertake this investigation which led him to discover a solution to the Einstein field equations [30], describing a spherically symmetric object embedded in an expanding universe. McVittie's solution has faced criticism involving the horizon structure and the nature of the central object, however, later it was realized that there were misstatements made about the metric [31 - 32] and there was a subtlety to understanding the space-time [33 - 34]. However, these controversies do not concern us in our investigation, we merely intend to use the McVittie space-time as a background to perform simple thought experiments that could directly detect the expansion of the universe by means of the holonomy produced by the metric. That is, the parallel transport of a

vector around a closed loop in a curved space-time, which would result in a deficit angle between the initial and final directions of the vector.

We carry out a similar investigation and analysis to that of Rothman, Ellis and Murugan [35], where the deficit angle produced for a variety of trajectories in the Schwarzschild-Droste static geometry was calculated. Instead, we carry this out for the McVittie metric.

In principle, any cosmological expansion should affect the deficit angle of a vector under parallel transport and this would allow direct experimental detection of the universe's expansion. However, we expect these effects to be incredibly small, as we have found, but are surprisingly large if it is compared to the LIGO measurement of the dimensionless strain of 10^{-21} – successfully measured.

5.1 The McVittie metric

The metric describing the McVittie space-time, in isotropic coordinates, is given by:

$$ds^2 = -\frac{\left(1-\frac{m_o}{2a(t)r}\right)^2}{\left(1+\frac{m_o}{2a(t)r}\right)^2}dt^2 + a(t)^2\left(1+\frac{m_o}{2a(t)r}\right)^4\left(dr^2+r^2d\Omega^2\right), \tag{5.1}$$

where m_o is the mass of the central object. The McVittie metric gives a general description of an expanding universe containing a central body. This can be seen by setting $a = 1$, which recovers the Schwarzschild metric, and $m_o = 0$ retrieves the flat FLRW space-time. In our chosen form of the metric, r represents a co-moving coordinate since the normalized 4-velocity is

$$u^a = \frac{\left[1+\frac{m_o}{2a(t)r}\right]}{\left[1-\frac{m_o}{2a(t)r}\right]}\delta^a{}_0. \tag{5.2}$$

So given a particle of mass m_o, it will follow the specified path r. This describes the average motion of matter at each space-time event, therefore if a light beam were sent along a circular orbit it could return to the original apparatus if r is constant but not if the proper distance $d(t) = ra(t)$ is constant. In the latter case,

the universe would have expanded during the transit time and the beam would return to a different device. Hence, the term "circular" refers to circular in co-moving coordinates (5.1)-(5.2), throughout this part of the dissertation. All calculations are performed in an orthonormal tetrad basis $\{e_a\}$ such that $e^a(e_b) = e^{(a)}{}_\mu e^\mu{}_{(b)} = \delta^{(a)}{}_{(b)}$. The dual basis 1-forms $\{\omega^a = \omega^{(a)}{}_\mu dx^\mu\}$, representing such a tetrad for our metric (5.1), are

$$\omega^0 = \omega^t = \frac{\left[1 - \frac{m_o}{2a(t)r}\right]}{\left[1 + \frac{m_o}{2a(t)r}\right]} dt, \tag{5.3}$$

$$\omega^1 = \omega^r = a(t)\left[1 + \frac{m_o}{2a(t)r}\right]^2 dr, \tag{5.4}$$

$$\omega^2 = \omega^\theta = a(t)\left[1 + \frac{m_o}{2a(t)r}\right]^2 r d\theta, \tag{5.5}$$

$$\omega^3 = \omega^\varphi = a(t)\left[1 + \frac{m_o}{2a(t)r}\right] r\sin\theta d\varphi. \tag{5.6}$$

The connection coefficients by the Cartan equation, $d\omega^a = -\omega^a{}_b \wedge \omega^b$, are

$$\omega^0{}_1 = \omega^1{}_0 = \frac{m_o}{a(t)^2 r^2 \left(1 + \frac{m_o}{2a(t)r}\right)^2 \left(1 - \frac{m_o^2}{4a(t)^2 r^2}\right)} \omega^0 + \frac{\dot{a}(t)}{a(t)} \omega^1, \tag{5.7}$$

$$\omega^0{}_2 = \omega^2{}_0 = \frac{\dot{a}(t)}{a(t)} \omega^2, \tag{5.8}$$

$$\omega^0{}_3 = \omega^3{}_0 = \frac{\dot{a}(t)}{a(t)} \omega^3, \tag{5.9}$$

$$\omega^2{}_1 = -\omega^1{}_2 = \frac{\left(1 - \frac{m_o}{2a(t)r}\right)}{a(t) r \left(1 + \frac{m_o}{2a(t)r}\right)^3} \omega^2, \tag{5.10}$$

$$\omega^3{}_1 = -\omega^1{}_3 = \frac{\left(1 - \frac{m_o}{2a(t)r}\right)}{a(t) r \left(1 + \frac{m_o}{2a(t)r}\right)^3} \omega^3, \tag{5.11}$$

$$\omega^2{}_3 = -\omega^3{}_2 = \frac{\cot\theta}{\left(1 + \frac{m_o}{2a(t)r}\right)^3} \omega^3. \tag{5.12}$$

The evolution equations of a vector with tetrad components A^a along a curve $x^b(\Lambda)$ with tangent vector $X^b(\Lambda) = dx^b/d\Lambda$ and curve parameter Λ are constructed from the parallel transport equation,

$$dA^a + \omega^a{}_b A^b = 0, \tag{5.13}$$

which yields

$$\begin{aligned}
&dA^t + \frac{m_o}{a^2 r^2 \left(1+\frac{m_o}{2ra}\right)^4} A^r dt + Ha\left(1+\frac{m_o}{2ra}\right)^2 A^r dr \\
&\quad + Har\left(1+\frac{m_o}{2ra}\right)^2 A^\theta d\theta + Har\left(1+\frac{m_o}{2ra}\right)^2 \sin\theta A^\phi d\phi = 0, \qquad (5.14)\\
&dA^r + \frac{m_o}{a^2 r^2 \left(1+\frac{m_o}{2ra}\right)^4} A^t dt + Ha\left(1+\frac{m_o}{2ra}\right)^2 A^t dr \\
&\quad - \frac{\left(1-\frac{m_o}{2ra}\right)}{\left(1+\frac{m_o}{2ra}\right)} A^\theta d\theta - \frac{\left(1-\frac{m_o}{2ra}\right)}{\left(1+\frac{m_o}{2ra}\right)} \sin\theta A^\phi d\phi = 0, \qquad (5.15)\\
&dA^\theta + Har\left(1+\frac{m_o}{2ra}\right)^2 A^t d\theta + \frac{\left(1-\frac{m_o}{2ra}\right)}{\left(1+\frac{m_o}{2ra}\right)} A^r d\theta \\
&\quad + \frac{\cos\theta(ar)}{\left(1+\frac{m_o}{2ra}\right)} A^\phi d\phi = 0, \qquad (5.16)\\
&dA^\phi + Har\left(1+\frac{m_o}{2ra}\right)^2 \sin\theta A^t d\phi + \frac{\left(1-\frac{m_o}{2ra}\right)}{\left(1+\frac{m_o}{2ra}\right)} \sin\theta A^r d\phi \\
&\quad - \frac{\cos\theta(ar)}{\left(1+\frac{m_o}{2ra}\right)} A^\theta d\phi = 0. \qquad (5.17)
\end{aligned}$$

In this construction, t is not an affine parameter, and it does not matter in our case as will be shown in the proceeding section.

Since the magnitude of the vectors A^a are conserved along any curve when parallel transported, we obtain a useful property:

$$-(A^t)^2 + (A^r)^2 + (A^\theta)^2 + (A^\phi)^2 = constant, \tag{5.18}$$

which will be used extensively in the coming sections.

5.2 Circular Holonomy

5.2.1 Geodesic orbits and Kepler's law

In this section, we lay down the foundations for our thought experiment. To measure the holonomy, we will consider vectors moving on a circular orbit in the equatorial plane. It should be noted that due to the McVittie space-time's feature of a nonzero pressure gradient, these circular orbits are not actual geodesics. Since there is an external force acting on a particle traveling on one of these orbits, it would spiral inward over an orbital period from a radius r_1 to r_2. This, of course, would result in the geodesics not being closed and in principle one could not measure the holonomy unless with the assistance of rockets to ensure that an apparatus is returned to its initial location. The other trouble would be that in order for an apparatus to follow a circular orbit, rockets would somehow have to hold it at a fixed radius. Having to use rockets in an experiment would be grossly unfeasible since this would introduce positioning errors and the desired result may not be reached.

However, over an orbital period, an apparatus can be allowed to freely follow a geodesic from r_1 to r_2. The difference between r_1 and r_2 in the McVittie space-time is so small that the error is negligible. So measuring the holonomy would be as if the apparatus were on a circular orbit. This approach is used in our thought experiments and it is shown that the error obtained in measuring the difference between r_1 and r_2 is indeed negligible.

Also, it should be noted that the formal definition for a geodesic is when the tangent vector to a curve remains parallel to itself. Thus, the geodesic equation with an arbitrary curve parameter, λ, and tangent vector X^a is given by

$$X^b \nabla_b X^a = f X^a, \tag{5.19}$$

where ∇_b is the differential operator.

When the proper time τ is the curve parameter, the function f is

$$f = \frac{d^2\lambda/d\tau^2}{(d\lambda/d\tau)^2} = 0, \tag{5.20}$$

since the proper time is an affine parameter.

If the coordinate time t is chosen as the curve parameter, and the radius r is constant, then the coordinate time t and proper time τ has the relation

$$d\tau = \frac{\left(1-\frac{k}{2a}\right)}{\left(1+\frac{k}{2a}\right)}dt, \tag{5.21}$$

where

$$^{\ddagger}k \equiv \frac{m_o}{r}. \tag{5.22}$$

From this, we find f to be

$$f = -\frac{Hk/a}{\left(1-\frac{k}{2a}\right)\left(1+\frac{k}{2a}\right)}. \tag{5.23}$$

The condition $f = 0$ is satisfied in the limiting cases of the McVittie space-time – when $a = 1$, which corresponds to the Schwarzschild case since $H = \dot{a}/a$, and when $k = 0$, which corresponds to the FLRW case. In the general case when H and k are nonzero, t is no longer an affine parameter. Nonetheless, the coordinate time t can still be used as the curve parameter along circular orbits since the parallel transport equation of the vector A^a moving in the equatorial plane will not change:

$$X^b \nabla_b A^a = 0. \tag{5.24}$$

Working with the coordinate time as the curve parameter instead would avoid having to perform complicated coordinate transformations and allow us to easily calculate the limiting cases. Now, as we have defined circular orbits, the comoving radial coordinate $r = constant$, which implies $dr = 0$, the radial component of the tangent vector will be zero,

---

‡This definition has no relation to the curvature k in Part I.

$$\{r = r_0\} \Rightarrow \{X^r = 0\} \Rightarrow \{dX^r = 0\}. \tag{5.25}$$

Also, by symmetry, since we are in the equatorial plane, we may set $\theta = \pi/2$, so

$$\{d\theta = 0\} \Rightarrow \{X^\theta = 0\} \Rightarrow \{dX^\theta = 0\}. \tag{5.26}$$

Thus, for the curve parameter t, the components of the tangent vector in the tetrad frame are

$$X^\mu = \frac{1}{\alpha}\left[\frac{\left(1-\frac{k}{2a}\right)}{\left(1+\frac{k}{2a}\right)}, 0, 0, ar\left(1+\frac{k}{2a}\right)^2 \Omega\right], \tag{5.27}$$

where the normalization factor, α, is found by setting $X_\mu X^\mu = -1$ and the angular velocity is defined by

$$\Omega \equiv \frac{d\phi}{dt}. \tag{5.28}$$

If we take X^a as the tangent vector, Eq. (5.15) gives a relation between the components X^t and X^ϕ:

$$X^\phi = \frac{k}{ra^2}\left(1-\frac{k}{2a}\right)^{-1}\left(1+\frac{k}{2a}\right)^{-3}\Omega^{-1}X^t. \tag{5.29}$$

Then from Eq. (5.27) and Eq. (5.29), we obtain Kepler's Third Law in the McVittie spacetime:

$$\Omega^2 = \frac{k}{a^3 r^2\left(1+\frac{k}{2a}\right)^6}, \tag{5.30}$$

except that these are not strictly geodesic orbits and since the scale-factor evolves in this space-time, the angular frequency Ω and as a result the angular momentum of an object would change as well on a circular orbit. Note that for the Schwarzschild case ($a = 1$), Ω is different from the *Newtonian* value of

$$\Omega_N \equiv \frac{\sqrt{k}}{r}, \tag{5.31}$$

by $k \sim 10^{-8}$ in Earth's vicinity.

5.2.2 Holonomy in gyroscopic spin

To directly measure the holonomy we propose placing a gyroscope in an orbit around a central mass in a McVittie space-time. If we consider how the scalar product of an arbitrary vector and tangent vector ($X^a A_a$) changes as it is parallel transported along a geodesic, by Eq. (5.19), we have

$$X^b \nabla_b (X^a A_a) = (X^a A_a) f, \tag{5.32}$$

and together with Eq. (5.24) implies that $X^a A_a = 0$. Hence, these vectors are perpendicular for any curve parameter at a point in space-time, and remains perpendicular at all points on the geodesic that passes through that point. Therefore, in principle, using a gyroscope would be the most viable instrument to measure the holonomy since the spin vector of the gyro, S^a, would always be held perpendicular to the tangent vector of the orbit X^a, such that $S_a X^a = 0$.
In our experimental set-up the comoving radial coordinate r is constant and $\theta = \pi/2$, as the spin vector is parallel transported along a circular orbit. This gives $dr = d\theta = 0$, and reduces the parallel transport equations, (5.14)–(5.17) to:

$$dS^t + \frac{k}{a^2 r \left(1+\frac{k}{2a}\right)^4} S^r dt + Har \left(1+\frac{k}{2a}\right)^2 S^\phi d\phi = 0, \tag{5.33}$$

$$dS^r + \frac{k}{a^2 r \left(1+\frac{k}{2a}\right)^4} S^t dt - \frac{\left(1-\frac{k}{2a}\right)}{\left(1+\frac{k}{2a}\right)} S^\phi d\phi = 0, \tag{5.34}$$

$$dS^\theta = 0, \tag{5.35}$$

$$dS^\phi + Har \left(1+\frac{k}{2a}\right)^2 S^t d\phi + \frac{\left(1-\frac{k}{2a}\right)}{\left(1+\frac{k}{2a}\right)} S^r d\phi = 0. \tag{5.36}$$

The four velocity for a circular orbit is given by Eq. (5.27), and together with the condition $S_a X^a = 0$ gives the relation between S^t and S^ϕ as

$$S^t = \frac{\left(1+\frac{k}{2a}\right)^3}{\left(1-\frac{k}{2a}\right)} ar\Omega S^\phi. \tag{5.37}$$

Using Kepler's third law in the McVittie space-time simplifies this relation to

$$S^t = \pm \frac{\sqrt{\frac{k}{a}}}{\left(1-\frac{k}{2a}\right)} S^\phi. \tag{5.38}$$

Since the spin vector S^a is spacelike – it is always perpendicular to the four velocity, it is useful to normalize it such that $S^a S_a = 1$. Due to the spherical symmetry of our experimental set-up we can take $S^\theta = 0$. Therefore we obtain the constraint, as from Eq. (5.18),

$$-(S^t)^2 + (S^r)^2 + (S^\phi)^2 = 1. \tag{5.39}$$

This constraint together with Eq. (5.38) reduces the number of independent equations to one. We are then only left with the evolution equation of S^r given by Eq. (5.34), and after substituting Eqs. (5.38) and (5.30) gives:

$$\frac{dS^r}{dt} \mp \frac{\left(1-\frac{2k}{a}+\frac{k^2}{4a^2}\right)\sqrt{\frac{k}{a}}}{ar\left(1-\frac{k}{2a}\right)\left(1+\frac{k}{2a}\right)^4} S^\phi = 0. \tag{5.40}$$

Now inserting Eq. (5.38) into the constraint, Eq. (5.39) gives

$$S^\phi = \pm \frac{\left(1-\frac{k}{2a}\right)}{\sqrt{1-\frac{2k}{a}+\frac{k^2}{4a^2}}} \sqrt{1-(S^r)^2}. \tag{5.41}$$

Substituting this expression into the evolution equation for S^r, Eq. (5.40), yields the decoupled differential equation:

$$\frac{dS^r}{dt} \mp \Psi(t)\sqrt{1-(S^r)^2} = 0, \tag{5.42}$$

where

$$\Psi(t) = \frac{\sqrt{\frac{k}{a}\left(1 - \frac{2k}{a} + \frac{k^2}{4a^2}\right)}}{ar\left(1 + \frac{k}{2a}\right)^4}. \tag{5.43}$$

This is straight-forward to integrate and its general solution is

$$S^r(t) = \mp \sin\left[c_1 + \int_{t_0}^{t} \Psi(t)dt\right]. \tag{5.44}$$

The solutions to the remaining spin vector components are then directly given by Eqs. (5.41) and (5.38):

$$S^\phi(t) = \mp \frac{\left(1 - \frac{k}{2a}\right)}{\sqrt{1 - \frac{2k}{a} + \frac{k^2}{4a^2}}} \cos\left[c_1 + \int_{t_0}^{t} \Psi(t)dt\right], \tag{5.45}$$

and

$$S^t(t) = \mp \frac{\sqrt{\frac{k}{a}}}{\sqrt{1 - \frac{2k}{a} + \frac{k^2}{4a^2}}} \cos\left[c_1 + \int_{t_0}^{t} \Psi(t)dt\right]. \tag{5.46}$$

These are the general solutions for S^a in the McVittie space-time.

In the Schwarzschild case ($a = 1$),

$$\Psi \equiv \Psi_0 = \frac{\sqrt{k\left(1 - 2k + \frac{1}{4}k^2\right)}}{r\left(1 + \frac{1}{2}k\right)^4} = constant. \tag{5.47}$$

In this special case, the spin vector components are:

$$S^t(t) = \mp \frac{\sqrt{k}}{\sqrt{1 - 2k + \frac{1}{4}k^2}} \cos\left[c_1 + \Psi_0(t - t_0)\right], \tag{5.48}$$

$$S^r(t) = \mp \sin\left[c_1 + \Psi_0(t - t_0)\right], \tag{5.49}$$

$$S^\phi(t) = \mp \frac{\left(1 - \frac{1}{2}k\right)}{\sqrt{1 - 2k + \frac{1}{4}k^2}} \cos\left[c_1 + \Psi_0(t - t_0)\right], \tag{5.50}$$

which oscillate with constant frequency Ψ_0. In contrast to the McVittie space-time, as $a \to \infty$, $\Psi \to 0$, meaning that the spin vectors would undergo damped

oscillations; S^r and S^ϕ become constant and S^t goes to zero.

In the following chapter we propose two feasible experiments.

6. Gedankenexperiment: Gyroscope Spin along Circular Geodesics

6.1 Experiment with one co-moving and one orbiting apparatus

Our first experiment involves two gyroscopes starting at point A (see Fig. 6.1), one which follows a circular path, Γ_1, of radius r_0, while the other follows a timelike path, Γ_2, at a constant comoving radius r_0 and constant angular coordinates θ_0, ϕ_0. N.B. this is not a geodesic and the assistance of a rocket engine would be needed to keep the instrument on its path.

Both gyroscopes would start at point A, at time $t = t_0$, and meet again at a point B at time $t = t_0 + t_{2\pi}$. We find the total holonomy by comparing the vector components at the point B where the two paths intersect again.

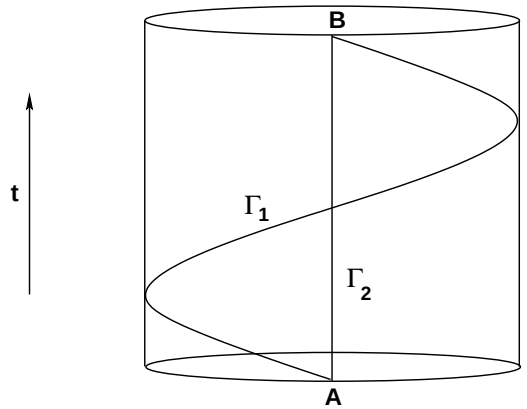

Figure 6.1: Visualization of the experiment.

Along the Γ_2 path, $dr = d\theta = d\phi = 0$, so for the spin vector along this path, the parallel transport equations are

$$dS_2^t + \frac{k}{a^2 r\left(1+\frac{k}{2a}\right)^4} S_2^r dt = 0, \tag{6.1}$$

$$dS_2^r + \frac{k}{a^2 r\left(1+\frac{k}{2a}\right)^4} S_2^t dt = 0, \tag{6.2}$$

$$dS_2^\theta = 0, \tag{6.3}$$

$$dS_2^\phi = 0. \tag{6.4}$$

Additionally, we have $X^a = [X^t, 0, 0, 0]$ along this path. Now, since $S_a X^a = 0$ we need $S_2^t = 0$ along the path. Setting $S_2^t = 0$ gives $S_2^r = constant$, from Eq. (6.2). This also means that $dS_2^t = 0$ which requires $S_2^r = 0$, from Eq. (6.1). Then with no loss of generality, $S^\theta = 0$, and the normalized spin vector along Γ_2 is the constant vector:

$$S_2^a(t) = [0, 0, 0, 1]. \tag{6.5}$$

Now starting with both devices at the same space-time point at $t = t_0$, the readings of their corresponding spin vectors are taken. The apparatus moving along the path Γ_1 will obey Eqs. (5.44)–(5.46). At the time t_0, we set $a(t_0) = 1$ and to obtain the appropriate initial conditions we choose $c_1 = \pi/2$. Then initially:

$$S_1^t(t_0) = \mp \frac{\sqrt{\frac{k}{a}}}{\sqrt{1 - \frac{2k}{a} + \frac{k^2}{4a^2}}} \cos\left[\frac{\pi}{2} + \int_{t_0}^{t_0} \Psi(t) dt\right] = 0, \tag{6.6}$$

$$S_1^r(t_0) = \mp \sin\left[\frac{\pi}{2} + \int_{t_0}^{t_0} \Psi(t) dt\right] = 1, \tag{6.7}$$

$$S_1^\phi(t_0) = \mp \frac{\left(1 - \frac{k}{2a}\right)}{\sqrt{1 - \frac{2k}{a} + \frac{k^2}{4a^2}}} \cos\left[\frac{\pi}{2} + \int_{t_0}^{t_0} \Psi(t) dt\right] = 0. \tag{6.8}$$

Thus, the spin measured at the initial time t_0 is:

$$S_1^a(t_0) = [0,1,0,0]. \tag{6.9}$$

At t_0, the difference in the spin of the two gyroscopes is
$S_1^a(t_0) - S_2^a(t_0) = [0,1,0,-1]$. This shows, clearly, that these vectors are perpendicular to each other.
Given the initial conditions, next we measure the spin at the final point B when the apparatus on the path Γ_1 has completed a full rotation and both apparatus coincide again. The time, $t_{2\pi}$, at which this point occurs can be found by solving for $t_{2\pi}$ from the expression for the angular frequency Ω:

$$2\pi = \frac{\sqrt{k}}{r}\int_{t_0}^{t_0+t_{2\pi}} \frac{dt}{a^{3/2}\left(1+\frac{k}{2a}\right)^3}. \tag{6.10}$$

At this point, we can see that the spin vectors of the two gyroscopes are no longer perpendicular to each other. Therefore, the net holonomy of S_1^a is given by

$$\Delta S_1^a = S_1^a(t_0+t_{2\pi}) - S_1^a(t_0). \tag{6.11}$$

If we consider an experiment which runs for less than cosmological times, from Eq. (5.43), we have, to the first order in k,

$$\Psi(t) = \frac{1}{a^{3/2}}\left(1-\frac{3k}{a}\right)\Omega_N. \tag{6.12}$$

For exponential expansion, $a = [(t_0+\Delta t)/t_0]^n$, with $\Delta t << t_0$, Eqs. (5.44)–(5.46) give, to first order in k,

$$S^t = \mp k^{1/2}\left(1+k-\frac{n\Delta t}{2t_0}\right)\cos\left[\frac{\pi}{2}+\left(1-3k-\frac{3}{4}\frac{n\Delta t}{t_0}\right)\Omega_N\Delta t\right], \tag{6.13}$$

$$S^r = \mp\sin\left[\frac{\pi}{2}+\left(1-3k-\frac{3}{4}\frac{n\Delta t}{t_0}\right)\Omega_N\Delta t\right], \tag{6.14}$$

$$S^\phi = \mp\left(1+\frac{k}{2}\right)\cos\left[\frac{\pi}{2}+\left(1-3k-\frac{3}{4}\frac{n\Delta t}{t_0}\right)\Omega_N\Delta t\right]. \tag{6.15}$$

In the case of de Sitter expansion, $a = e^{Ht}$, with $Ht << 1$:

$$S^t = \mp k^{1/2}\left(1+k-\frac{Ht}{2}\right)\cos\left[\frac{\pi}{2}+\left(1-3k-\frac{3}{4}Ht\right)\Omega_N t\right], \tag{6.16}$$

$$S^r = \mp\sin\left[\frac{\pi}{2}+\left(1-3k-\frac{3}{4}Ht\right)\Omega_N t\right], \tag{6.17}$$

$$S^\phi = \mp\left(1+\frac{k}{2}\right)\cos\left[\frac{\pi}{2}+\left(1-3k-\frac{3}{4}Ht\right)\Omega_N t\right]. \tag{6.18}$$

In this approximation, we may take the Newtonian value of $t_{2\pi}$ as $t_{2\pi} = 2\pi r k^{-1/2}$, in which $\Omega_N t$ becomes 2π. If we take the initial time as $t_0 = 0$ then the holonomy for the spin components is then $\Delta S^a(t_{2\pi}) - S^a(0)$. We find the holonomy for the spin components in the de Sitter case, to the lowest order in k, is

$$\Delta S^t = 6\pi k^{3/2} + 3\pi^2 Hr, \tag{6.19}$$

$$\Delta S^r = 18\pi^2 k^2 + 18\pi^3 k^{1/2} Hr, \tag{6.20}$$

$$\Delta S^\phi = 6\pi k + \frac{3\pi^2 Hr}{k^{1/2}}, \tag{6.21}$$

with similar expressions for the power-law expansion. Later we will see that there is no difference in these two cases of universal expansion by numerical solutions. In an orbit of 1AU, $k \approx 10^{-8}$ and $Hr \approx 10^{-15}$, the holonomy for all the components after a single rotation is

$$\Delta S^a \sim [10^{-11}, 10^{-14}, 0, 10^{-7}]. \tag{6.22}$$

A rather useful quantity to compute is how much the McVittie space-time deviates from the Schwarzschild geometry. The first term in each of the expressions above is the holonomy produced in the Schwarzschild case, which is independent of H. Therefore, the fractional deviation of McVittie from Schwarzschild is

$$f^a = \frac{\Delta S^a_S - \Delta S^a_{McV}}{\Delta S^a_S}, \tag{6.23}$$

where the expression for each component is:

$$f^t = \frac{\pi H r}{2k^{3/2}} \sim 10^{-3}, \tag{6.24}$$

$$f^r = \frac{\pi H r}{k^{3/2}} \sim 10^{-3}, \tag{6.25}$$

$$f^\phi = \frac{\pi H r}{2k^{3/2}} \sim 10^{-3}. \tag{6.26}$$

The numerical calculation of the fractional deviation in the space-times is tabulated in Table 6.1.

f^a	**Schwarzschild**	**McVittie**	**Fractional Deviation**
f^t	1.885×10^{-11}	1.888×10^{-11}	-1.592×10^{-3}
f^r	-1.776×10^{-14}	-1.787×10^{-14}	-6.194×10^{-3}
f^ϕ	1.885×10^{-7}	1.888×10^{-7}	-1.592×10^{-3}

Table 6.1: Fractional deviation of the Schwarzschild geometry from the McVittie space-time for the de Sitter case when $c_1 = \pi/2$.

In principle, the holonomy produced in this experiment is detectable with advanced enough technology since there is the problem of keeping the *stationary* observer at the same comoving radius. This could make the experiment next to impracticable and close to impossible. Next, we turn to a simpler proposal.

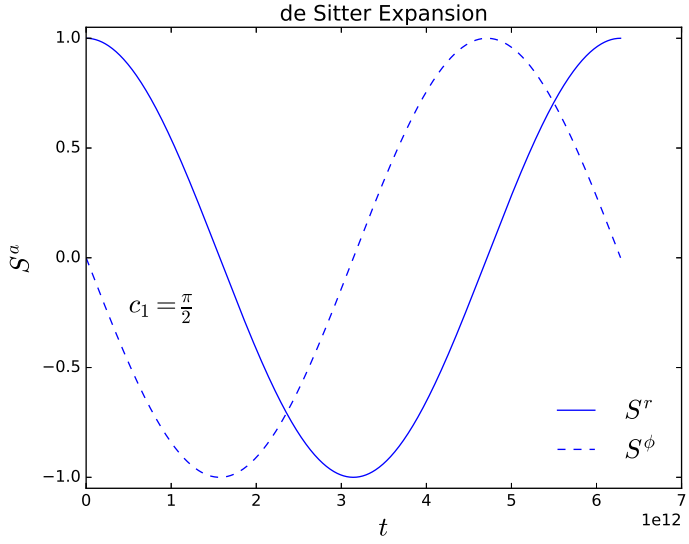

Figure 6.2: Numerical solution for the de Sitter case.

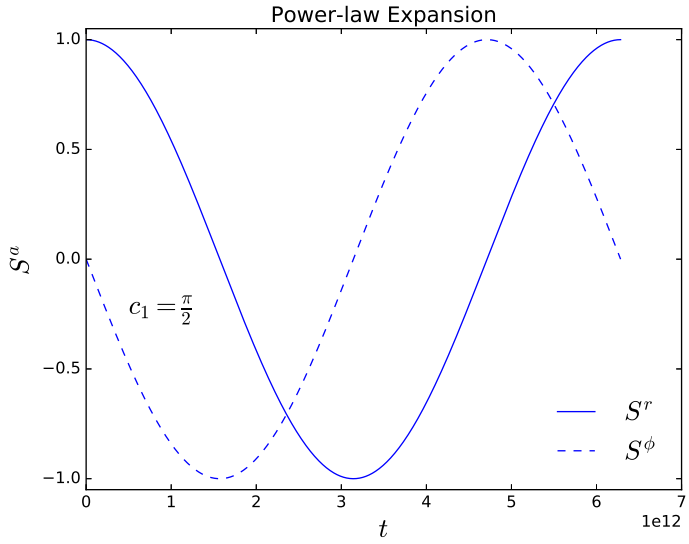

Figure 6.3: Numerical solution for the power-law case.

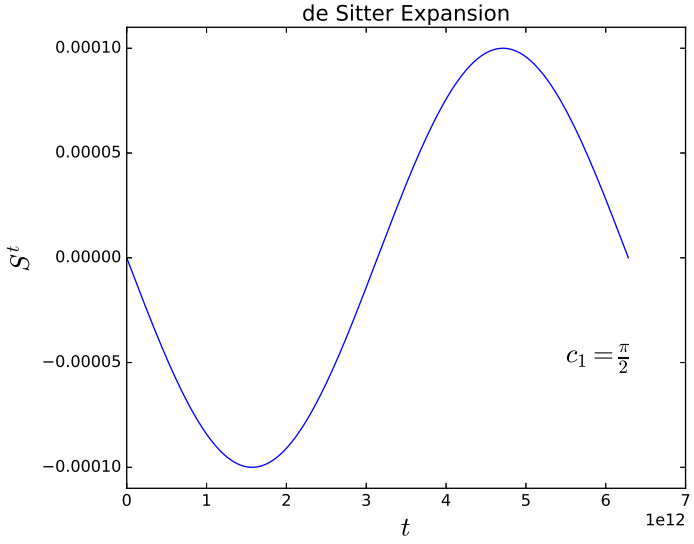

Figure 6.4: Numerical solution for the temporal component of the spin vector in the de Sitter case.

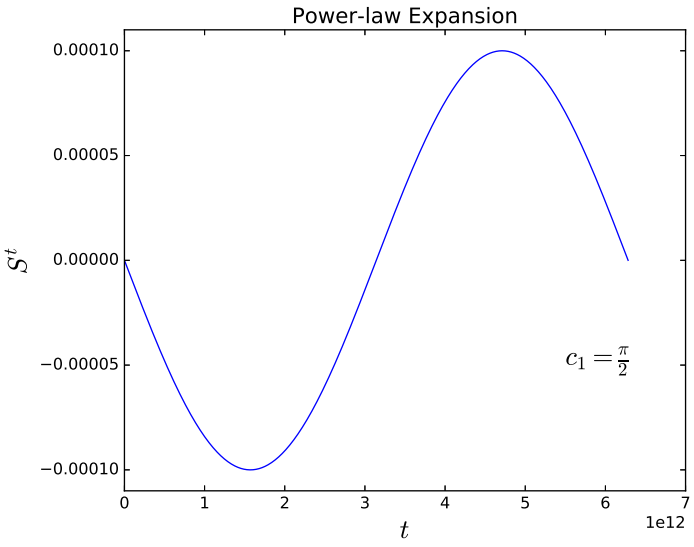

Figure 6.5: Numerical solution for the temporal component of the spin vector in the power-law case.

6.2 Experiment with two counter-orbiting gyroscopes

To reiterate, measuring the holonomy, the components of the tangent vector are compared after the instrument or particle has traveled a closed path. So a comparison cannot be made using only a single instrument because after one orbit it is no longer in its original space-time position; this is not even possible in the Schwarzschild universe.

However, one can imagine two apparatus with their spin vectors aligned at an initial time $t = 0$. Then they are sent on circular orbits but in the opposite directions through an angle of 2π, meeting again at the antipodal point which would be the same comoving observation point. Since the magnitude of the angular frequency, Ω, is the same for both apparatus but with opposite signs at each point, the change in the vector components will add. So the total holonomy of each apparatus will be half of their sum.

The geometrical interpretation of this is as follows:

Initially, the spin vectors are $S^a(t_0) = [S^t(t_0), S^r(t_0), 0, S^\phi(t_0)]$, and at the antipodal point when $t = t_{2\pi}$ the vectors become $S^a(t_{2\pi}) = [S^t(t_{2\pi}), S^r(t_{2\pi}), 0, S^\phi(t_{2\pi})]$. This shows that there is a boost in two different directions relative to the tetrad frame because the magnitudes of the spin vectors remain constant (by (5.18)), and hence is a Lorentz transformation. So the sum of the boosts represents a rotation, since $S^\theta = 0$, the net change in the spatial part of the spin vector lies in the (r, ϕ) plane, i.e. the θ direction.

The change in the spin vectors is the same as in the previous experiment, in the last section, but in this case the net holonomy change is $2\Delta S^a$. Therefore, on the scale of the solar system, there is no difference between the two universal expansions – de Sitter and power law, and the order of magnitude of the net holonomy is the same as before $\Delta S^a \sim [10^{-11}, 10^{-14}, 0, 10^{-7}]$.

We remind that circular orbits in the McVittie space-time are not actual geodesics, as explained before. However, the error obtained by assuming circular orbits is

negligible. For example, we found in the de Sitter case with $k \equiv m_o/r$ and $c_1 = \pi/2$, that

$$\Delta S^r = 18\pi^2 k^2 + 18\pi^3 k^{1/2} Hr, \tag{6.27}$$

for a circular orbit.

If we take two circular orbits of radii r_2 and r_1, the fractional change would be

$$f_1 = \frac{\Delta S^a(r_1)_S - \Delta S^a(r_1)_{McV}}{\Delta S^a(r_1)_S}, \tag{6.28}$$

$$f_2 = \frac{\Delta S^a(r_2)_S - \Delta S^a(r_2)_{McV}}{\Delta S^a(r_2)_S}. \tag{6.29}$$

Now if we use r_2 instead of r_1 to measure the fractional change in these space-times, gives:

$$\Delta f = \frac{f_2 - f_1}{f_1}. \tag{6.30}$$

To the lowest approximation, McVittie shows, using our notation that:

$$\frac{1}{r} = \frac{m_o a(t)}{h^2}, \tag{6.31}$$

where h is some constant. If we choose $a_0 = a(0) = 1$, this corresponds to the value of the scale-factor set to today, then:

$$\frac{1}{r_1} = \frac{m_o}{h^2}. \tag{6.32}$$

Using $\Delta r \equiv r_2 - r_1$, we have for de Sitter expansion $a = e^{Ht}$:

$$-\frac{\Delta r}{r_1} = H\Delta t << 1. \tag{6.33}$$

Equations (6.27) and (6.30) then give:

$$\Delta f^r = 2H\Delta t = \frac{4\pi H r_1}{k^{1/2}}, \tag{6.34}$$

to the lowest order and assuming a Newtonian time $t = 2\pi r k^{-1/2}$. This has a value of $\sim 10^{-10}$. Hence, the error in computing the holonomy by ignoring the difference between r_2 and r_1 is negligible.

7. Discussion

Two simple thought experiments have been discussed which, in principle, could be performed with advanced enough technology. However, the outcome of these experiments depends on the scale at which virialization occurs as structure formation takes place. So the experiments would have to be carried out on the scale of galaxy clusters, in principle. Regardless, it is interesting to consider experiments that show effects on the scale of the solar system, assuming that the solar system is embedded in an expanding universe, which the McVittie metric has enabled to do and allow us to calculate the holonomy produced by the gyroscopes. We note that the main difference between a Schwarzschild and McVittie geometry is the variation in both the frequency and amplitude of the gyroscope's spin vector seen in the McVittie case.

Comparing the fractional change in these two spacetimes, only the time component of the spin vector has a significant change which has a measured holonomy of $\sim 10^{-11}$. However, on the scale of our solar system, distinguishing between the two geometries would not be possible since the virialization scale is much larger. Nonetheless, this proposal is interesting in the context of how the universe on large scales influence local physics, as previously investigated by Einstein and Strauss [26], and Noerdlinger and Petrosian [36].

8. Conclusions

In the first part of the dissertation, we explored how a cyclic universe can be achieved in a Friedmann cosmology. We proposed replacing the cosmological constant with a decaying term in the Friedmann equations and coupling the Friedmann model to a scalar field produces cyclic solutions in its phase space. Modeling the early universe with a single scalar field and adding a damping term to the Klein Gordon equation to simulate reheating, it was found that there is a violation of the energy condition, $|w_{eff}| > 1$, when the dynamical evolution returns to the bounce in the early universe which goes through a contracting phase. Including the process of reheating in cyclic models of the universe have not been covered in the literature before and provides a new insight into these models in cosmology.

Contrary to other complex models, e.g. the ones using M-theory to produce cyclic behaviour or show that our universe could undergo a bounce, our model has the simple condition that $w_{eff} < -1/3$ and at some point in the future evolution of our universe that dark energy decays in the Friedmann cosmology which is also currently regarded as the best model describing our universe from the radiation epoch up until today.

Since we would like to describe the universe as accurately and detailed as possible, including the process of reheating to this model might jeopardize the idea of cyclic cosmology. However, the process of reheating is not completely understood and it would be interesting to explore other models of reheating in the context of cyclic cosmology as future work.

In the second part, we measured the holonomy produced by a universe which

behaves like the McVittie spacetime. Circular orbits are assumed where the error obtained is negligible on the scales we are performing our experiments. The computed holonomy in the two experiments considered are of the same order of magnitude, $\Delta S^a \sim [10^{-11}, 10^{-14}, 10^{-7}]$, where the choice for the initial condition $c_1 = \pi/2$ gives a normalized initial spin vector $S_1^a(t_0) = [0,1,0,0]$ as in Eq. (6.9) which would be much easier to set-up experimentally.

However, as discussed in the previous section, these experiments would have to be performed on the scale of galaxy clusters due to virialization. Regardless, it is interesting to show these effects on the scale of our solar system, assuming a McVittie geometry, and also to see how the large scale universe affects the local physics.

Bibliography

[1] M. Goliath and G. F. R. Ellis. Homogeneous cosmologies with a cosmological constant. *Physical Review D*, 60(2):023502, 1999.

[2] P. A. R. Ade et al. Planck 2015 results. XX. Constraints on inflation. *Astronomy and Astrophysics*, 594:A20, 2016.

[3] Planck Collaboration, Y. Akrami, et al. Planck 2018 results. X. Constraints on inflation. *arXiv e-prints*, page arXiv:1807.06211, 2018.

[4] R. C. Tolman and M. Ward. On the behavior of non-static models of the universe when the cosmological term is omitted. *Physical Review*, 39(5):835, 1932.

[5] I. B. Zeldovich and I. D. Novikov. *Relativistic astrophysics. Volume 2 - The structure and evolution of the universe*. Chicago, IL, University of Chicago Press, 1983.

[6] L. Parker and S. A. Fulling. Quantized matter fields and the avoidance of singularities in general relativity. *Physical Review D*, 7:2357–2374, 1973.

[7] A. G. Riess, A. V. Filippenko, P. Challis, A. Clocchiatti, A. Diercks, P. M. Garnavich, R. L. Gilliland, C. J. Hogan, S. Jha, R. P. Kirshner, et al. Observational evidence from supernovae for an accelerating universe and a cosmological constant. *The Astronomical Journal*, 116(3):1009, 1998.

[8] J. D. Barrow and M. P. Dabrowski. Oscillating Universes. *Monthly Notices of the Royal Astronomical Society*, 275:850, 1995.

[9] J. Khoury, B. A. Ovrut, P. J. Steinhardt, and N. Turok. The Ekpyrotic universe: Colliding branes and the origin of the hot big bang. *Physical Review D*, 64:123522, 2001.

[10] A. Linde. Inflationary Cosmology after Planck 2013. In *Proceedings, 100th Les Houches Summer School: Post-Planck Cosmology: Les Houches, France*, pages 231–316, 2015.

[11] R. Kallosh, L. Kofman, and A. D. Linde. Pyrotechnic universe. *Physical Review D*, 64:123523, 2001.

[12] R. Kallosh, L. Kofman, A. D. Linde, and A. A. Tseytlin. BPS branes in cosmology. *Physical Review D*, 64:123524, 2001.

[13] A. Ijjas. Cyclic completion of the anamorphic universe. *Classical and Quantum Gravity*, 35(7):075010, 2018.

[14] P. J. Steinhardt and N. Turok. A cyclic model of the universe. *Science*, 296(5572):1436–1439, 2002.

[15] G. F. R. Ellis and R. Maartens. The emergent universe: Inflationary cosmology with no singularity. *Classical and Quantum Gravity*, 21:223–232, 2004.

[16] G. F. R. Ellis, J. Murugan, and C. G. Tsagas. The Emergent universe: An Explicit construction. *Classical and Quantum Gravity*, 21(1):233–250, 2004.

[17] K. Atazadeh and F. Darabi. Einstein static universe from GUP. *Physics of the Dark Universe*, 16:87–93, 2017.

[18] J. Liu, Y.-F. Cai, and H. Li. Evidences for bouncing evolution before inflation in cosmological surveys. *Journal of Theoretical Physics 1*, 2012.

[19] J. D. Barrow and C. Ganguly. Cyclic Mixmaster Universes. *Physical Review D*, 95(8):083515, 2017.

[20] D. Solomons, P. K. S. Dunsby, and G. F. R. Ellis. Bounce behaviour in Kantowski-Sachs and Bianchi cosmologies. *Classical and Quantum Gravity*, 23:001, 2006.

[21] P. A. R. Ade et al. Planck 2015 results. XIII. Cosmological parameters. *Astronomy and Astrophysics*, 594:A13, 2016.

[22] G. F. R. Ellis, E. Platts, D. Sloan, and A. Weltman. Current observations with a decaying cosmological constant allow for chaotic cyclic cosmology. *Journal of Cosmology and Astroparticle Physics*, 2016(04):026, 2016.

[23] A. H. Guth. Inflationary universe: A possible solution to the horizon and flatness problems. *Physical Review D*, 23(2):347, 1981.

[24] E. W. Kolb and M. S. Turner. The Early Universe. *Frontiers of Physics*, 69:1–547, 1990.

[25] T. Rothman, M. Campbell, R. Goswami, and G. F. R. Ellis. Direct Detection of Universal Expansion by Holonomy in the McVittie Spacetime. *Physical Review D*, 99:024033, 2019.

[26] A. Einstein and E. G. Straus. The influence of the expansion of space on the gravitation fields surrounding the individual stars. *Reviews of Modern Physics*, 17:120–124, 1945.

[27] I. Bochicchio and V. Faraoni. Cosmological expansion and local systems: a Lemaître-Tolman-Bondi model. *General Relativity and Gravitation*, 44:1479–1487, 2012.

[28] V. Faraoni and A. Jacques. Cosmological expansion and local physics. *Physical Review D*, 76:063510, 2007.

[29] F. I. Cooperstock, V. Faraoni, and D. N. Vollick. The Influence of the Cosmological Expansion on Local Systems. *The Astrophysical Journal*, 503:61–66, 1998.

[30] G. C. McVittie. The mass-particle in an expanding universe. *Monthly Notices of the Royal Astronomical Society*, 93:325–339, 1933.

[31] B. C. Nolan. A point mass in an isotropic universe: Existence, uniqueness, and basic properties. *Physical Review D*, 58:064006, 1998.

[32] B. C. Nolan. A point mass in an isotropic universe: III. The region R less than or = to 2m. *Classical and Quantum Gravity*, 16:3183–3191, 1999.

[33] N. Kaloper, M. Kleban, and D. Martin. McVittie's Legacy: Black Holes in an Expanding Universe. *Physical Review D*, 81:104044, 2010.

[34] K. Lake and M. Abdelqader. More on McVittie's legacy: A Schwarzschild – de Sitter black and white hole embedded in an asymptotically ΛCDM cosmology. *Physical Review D*, 84:044045, 2011.

[35] T. Rothman, G. F. R. Ellis, and J. Murugan. Holonomy in the Schwarzschild-Droste geometry. *Classical and Quantum Gravity*, 18:1217–1234, 2001.

[36] P. D. Noerdlinger and V. Petrosian. The Effect of Cosmological Expansion on Self-Gravitating Ensembles of Particles. *The Astrophysical Journal*, 168:1, 1971.

[37] K. Inomata, M. Kawasaki, K. Mukaida, and T. T. Yanagida. Double inflation as a single origin of primordial black holes for all dark matter and ligo observations. *Physical Review D*, 97(4):043514, 2018.

[38] J. Khoury, P.J. Steinhardt, and N. Turok. Designing cyclic universe models. *Physical Review Letters*, 92:031302, 2004.

[39] P. J. Steinhardt and N. Turok. The cyclic model simplified. *New Astronomy Reviews*, 49(2):43–57, 2005.

[40] D. Battefeld and P. Peter. A Critical Review of Classical Bouncing Cosmologies. *Physics Reports*, 571:1–66, 2015.

[41] M. Shinji. Hořava-Lifshitz cosmology: a review. *Classical and Quantum Gravity*, 27(22):223101, 2010.

[42] S. W. Hawking and R. Penrose. The singularities of gravitational collapse and cosmology. *Proceedings of the Royal Society of London A: Mathematical, Physical and Engineering Sciences*, 314(1519):529–548, 1970.

[43] A. Borde and A. Vilenkin. Eternal inflation and the initial singularity. *Physical Review Letters*, 72:3305–3309, 1994.

[44] G. F. R. Ellis, S. J. Stoeger, R. William, P. McEwan, and P. Dunsby. Dynamics of inflationary universes with positive spatial curvature. *General Relativity and Gravitation*, 34:1445–1459, 2002.

[45] A. D. Linde. Can we have inflation with $\Omega > 1$? *Journal of Cosmology and Astroparticle Physics*, 0305:002, 2003.

[46] R. M. Wald. Asymptotic behavior of homogeneous cosmological models in the presence of a positive cosmological constant. *Physical Review D*, 28:2118–2120, 1983.

[47] R. Brandenberger and P. Peter. Bouncing Cosmologies: Progress and Problems. *Foundations of Physics*, 47(6):797–850, 2017.

[48] T. Clifton and J. D. Barrow. The ups and downs of cyclic universes. *Physical Review D*, 75:043515, 2007.

[49] J. D. Barrow and D. Sloan. Bouncing Anisotropic Universes with Varying Constants. *Physical Review D*, 88:023518, 2013.

[50] J. D. Barrow and C. Ganguly. The Shape of Bouncing Universes. *International Journal of Modern Physics D*, 26:1743016, 2017.

[51] S. Carloni, P. K. S. Dunsby, and D. M. Solomons. Bounce conditions in f(R) cosmologies. *Classical and Quantum Gravity*, 23:1913–1922, 2006.

[52] A. A. Starobinskii. On a nonsingular isotropic cosmological model. *Soviet Astronomy Letters*, 4:82–84, 1978.

[53] Y. B. Zeldovich and A. A. Starobinsky. Particle production and vacuum polarization in an anisotropic gravitational field. *Journal of Experimental and Theoretical Physics*, 34:1159–1166, 1972. [Zh. Eksp. Teor. Fiz.61,2161(1971)].

[54] B. C. Nolan. A point mass in an isotropic universe: II. Global properties. *Classical and Quantum Gravity*, 16:1227–1254, 1999.

[55] H. B. G. Casimir and D. Polder. The influence of retardation on the London-van der Waals Forces. *Physical Review*, 73:360–372, 1948.

[56] S. M. Carroll. The cosmological constant. *Living Reviews in Relativity*, 4:1, 2001.